

DESIGN OF A LOW RADAR CROSS-SECTION RIG FOR CONTROLLED MOTION OF A CALIBRATED RADAR TARGET



Presented by:

Akhile Ngwenya

Prepared for:

Dr Francois Schonken

November 7, 2021

Submitted to the Department of Electrical Engineering at the University of Cape Town in partial fulfilment of the academic requirements for the degree of Mechatronics engineering.

Abstract

In this work we describe a novel Thesis Template, to be used by students in Electrical & Engineering at the University of Cape Town. This section entails the abstract of the document.

The project is an investigation into designing and prototyping a test rig to test the functionality of a RADAR system. There is minimal research that investigates the development of test rigs for radar systems, thus this provides an opportunity for novel designs. This thesis will aim to investigate possible designs and implement the designs. And collect data for analysis and discussion. The reason may provide a new methodology in testing radar systems using the theory in this thesis.

Acknowledgments

I would like to thank mu mother, my little bother, all of my friends from home for providing me with much needed support. I would also like to that my supervisor Dr. Francious Schonken for guiding me through this journey. And finally i would like to thank my father, who is no longer with me but his lessons have stuck with me, I hope to make him proud one day.

Plagiarism Declaration

1. I know that plagiarism is wrong. Plagiarism is to use another's work and pretend that it is one's own.
2. I have the IEEE convention for citation and referencing. Each contribution to, and quotation in, this final year project report from the work(s) of other people, has been attributed and has been cited and referenced.
3. This final year project report is my own work.
4. I have not allowed, and will not allow, anyone to copy my work with the intention of passing it off as their own work or part thereof.

.....

Akhile Ngwenya

November 7, 2021

Contents

Abstract	i
Acknowledgments	ii
Plagiarism Declaration	iii
Table of Contents	iv
List of Figures	viii
List of Tables	xii
Nomenclature	xiii
Chapter 1: Introduction	1
1.1 Introduction	1
1.2 Motivation	2
1.3 Problem Statement	2
1.4 Objectives	3
1.5 Contributions	4
1.6 Plan of development	4
1.7 Scope and Limitations	5
1.8 Outline	5

Chapter 2: Literature Review	7
2.1 Literature Review	7
2.2 Motor Theory	8
2.2.1 Servo motor	9
2.2.2 Stepper motor	10
2.2.3 BLDC motor	10
2.3 Position and velocity sensing tools	11
2.3.1 Hall effect sensor	11
2.3.2 Tachometers	12
2.3.3 Rotary encoder	12
2.4 Robots with lifting mechanisms	13
2.4.1 Predetermined motion planning for wheeled robots with arms for object	13
2.4.2 Hybrid Serial-Parallel Mobile Robot	15
2.5 Possilble Control methods	17
2.5.1 PID Control	17
2.5.2 Sliding Mode control	19
Chapter 3: Methodology	21
3.1 Problem identification	21
3.2 System Requirements	22
3.3 Requirement analysis	22
3.3.1 Analysis of S.R.001	22
3.3.2 Analysis of S.R.002	23
3.3.3 Analysis of S.R.003	24
3.3.4 Analysis of S.R.004	24
3.3.5 Analysis of S.R.005	25
3.4 Verification	25

3.5	Design Process	27
3.5.1	V-model Design process	27
Chapter 4:	Design	29
4.1	System Design	30
4.2	Hardware Design	31
4.2.1	Components Chosen	31
4.2.2	External Rig Design	35
4.2.3	Electrical Component layout design	44
4.3	Software Design	46
4.3.1	Motor Drive System	47
4.3.2	Lifting mechanism software design	65
4.4	Implementation	67
4.5	Testing	69
4.5.1	Motor System Testing	69
4.5.2	Lifting Mechanism Testing	70
Chapter 5:	Results	71
5.1	Results	71
5.2	No-load testing	71
5.2.1	Open loop Motor system testing results	72
5.2.2	closed loop Motor system testing results	78
5.2.3	Lifting mechanism testing results	84
5.3	Loaded Testing	84
5.3.1	Loaded Motor system testing results	85
5.3.2	Loaded Lifting mechanism testing results	89
5.4	Discussion	91
5.4.1	No load test results	91

5.4.2	Loaded Tests	93
Chapter 6:	Conclusions	94
6.1	Conclusions	94
6.2	Future Work	95
Bibliography		97
Appendix A:	Supporting Data	100
A.1	Electrical Hardware Connections	100
A.2	Encoder Internal circuitry	102
A.3	Encoder-Motor Setup	102
A.4	Modelling DC Motor	104
A.4.1	Deadzone code	104
A.4.2	Step input	106
A.5	Distance covered by rig code snippet	107
A.6	Lifting Mechanism Code snippet	109

List of Figures

1.1	Gantt chart for the project	4
2.1	Stator and Rotor of motor	9
2.2	Block diagram of servo motor feedback	10
2.3	Internal circuitry of hall effect sensor	11
2.4	Autonomous WMR	14
2.5	the model of the robot	16
3.1	V-model of the project	28
4.1	OPM Diagram of the basic operation of the rig	30
4.2	The servo motor with the dimensions	32
4.3	The arduino UNO R3 and schematic	33
4.4	DC motor	33
4.5	Encoder	34
4.6	Motor Driver	35
4.7	12V battery	35
4.8	The isometric and top view of the lower platform	36
4.9	Lower Platform profile	37
4.10	The isometric and top view of the upper platform	37
4.11	Upper Platform profile	38
4.12	The isometric and profile view of the lifting arm	38

4.13	The isometric and profile view of the lifting mechanisms	39
4.14	Diagram of the dimensions of the lifting platform	39
4.15	Diagram the scissor lift in its lowest height setting	40
4.16	The isometric and profile view of the Pulley system	41
4.17	The isometric and profile view of the servo motor housing	41
4.18	The isometric and profile view of the Motor holder	42
4.19	The isometric and profile view of the Back Wheel design	42
4.20	The isometric and profile view of front wheel shaft housing	43
4.21	The isometric and profile view of the Front Wheel design	43
4.22	Diagram of the electrical connections of the Motor Drive system	44
4.23	Diagram of the Slotted disk	45
4.24	Diagram of the Encoder-Disk configuration	45
4.25	Diagram of electrical connections for Lifting mechanism	46
4.26	Flowchart of the software design	47
4.27	Oscilloscope reading of the PWM pin	53
4.28	Figure of PWM values against rotational speed	54
4.29	The initial and final values of the step input	54
4.30	Rotational speed vs time graph	55
4.31	fitted Rotational speed vs time graph	56
4.32	The simulation of the plant and step response	58
4.33	Closed loop step response	59
4.34	Closed loop step PID response	62
4.35	Closed loop step GAin controller response	63
4.36	Line aprroximation of PWM(50-80) values and rotational velocity . .	64
4.37	Line aprroximation of PWM(80-250) values and rotational velocity .	64
4.38	Bottom platform with the Wheels attached	68
4.39	Lazercut Slot	68

4.40	Top platform and links	68
4.41	Line approximation of PWM(80-250) values and rotational velocity .	69
4.42	The set up for testing servo motors	70
5.1	The experimental set up for no-load motor subsystem testing	72
5.2	Run 1 experiment speed and distance travelled figure	73
5.3	Run 2 experiment speed and distance travelled figure	74
5.4	Run 3 experiment speed and distance travelled figure	75
5.5	Run 4 experiment speed and distance travelled figure	76
5.6	The isometric and profile view of front wheel shaft housing	76
5.7	Run 1 of proportional controller Speed and distance	79
5.8	Run 2 of proportional controller Speed and distance	80
5.9	Run 3 of proportional controller Speed and distance	80
5.10	Run 4 of proportional controller Speed and distance	81
5.11	Run 5 of proportional controller Speed and distance	82
5.12	Run 5 of proportional controller Speed and distance	83
5.13	Design of the Arm	86
5.14	illustration of teh configuration	86
5.15	Measuring the torque	87
5.16	Connection of the batteries and the motors	88
5.17	Pulleys connected to the lifting mechanism	89
5.18	Structural failure in the lifting mechanism	90
A.1	Diagram of electrical connections for Lifting mechanism	102
A.2	Diagram of electrical diagram of DC motor	104
A.3	Ethics	110

List of Tables

3.1	Table of System Requirements	22
3.2	Functional Requirements table	23
3.3	Functional requirements from S.R.002	23
3.4	Functional requirements from S.R.003	24
3.5	Functional requirements from S.R.004	24
3.6	Functional requirements from S.R.005	25
3.7	Verification table	26
5.1	Table of input and output speeds	77
5.2	input distance and distance travelled	78
5.3	Distance travelled and distance input	82
5.4	Speed of the motors in km/h	91
A.1	A table of corresponding electrical connections	101

Nomenclature

F.R Functional Requirements. [22](#)

OPM Object Process Methodology. [viii, 30](#)

PWM Pulse width modulation. [9](#)

R.V Requirement verification. [25](#)

S.R System Requirements. [22](#)

Chapter 1

Introduction

1.1 Introduction

When products or machinery are manufactured. They need to be tested to ensure they operate as intended, for instance when a car is built, one of the many tests performed is testing its performance in terms of power. The power is measured horsepowers, and how that is tested is by placing the car's engine in a dyno tester. This tester checks if the engine performs up to the rated horsepower. To test this accurately, the dyno has to be a reliable rig, meaning the performance of the dyno is just as important. The point is that, testing products is integral, which means the testing rigs must accurate and liable.

This brings us to the project which is to design a low radar cross-section rig for controlled motion of a calibrated radar target. In other words, a testing rig that will be used to test RADAR. The testing rig has to be mobile on a flat surface(asphalt) or on a track, and the testing rig must be able to carry light-weight metallic objects. These are some of the objectives that the rig must accomplish which will be discussed in details on later chapters. The background of this study is very limited because

this research is heavily design orientated, therefore there is no extensive research in the particular topic

1.2 Motivation

The motivation of the research is to have an accurate and testing rig for RADAR. It is well known that RADAR technologies are used in a plethora of industries from the manufacturing of cars to military use. It is an important piece of technology. Ensuring that the RADAR operates as intended is crucial because the cost of failure in the event a RADAR system was not tested properly and as a consequence, it does not operate correctly and that failure can have adverse effects. For instance if the radar systems in a car do not work properly they may cause car accidents to occur because the car could not accurately scan for any cars that would be close to the car. This example alone shows the importance of testing radar systems, thus building a testing rig is just as crucial.

The impact the research will have is that there will be a low cost, reliable, accurate and mobile testing rig which various products that use radar technology. The industry in this type of technology is very new, therefore there is a significant amount of potential for the research to progress far beyond the scope of this current research.

1.3 Problem Statement

Testing radar technology is essential, there is a need for a mobile testing rig to test the tracking performance of radar.

1.4 Objectives

The aim of the research, as described partially above, is to design and build a low radar cross-section rig for controlled motion of a calibrated radar target.

- Be able to carry light weight metallic objects e.g., polystyrene ball with a foil cover
- It must be able to move on a flat surface or track up to 50m in distance.
- Be able to Alternate height up to 2m

Expanding on the first point, the rig has to be designed in a manner that will be able to carry the objects, whether be able to grip the test objects with a manipulator such as a robot arm or, be design a platform in which the test objects will be placed on the platform.

With regard to the second point. The rig has to be able to move on a flat surface, for example, on the road to move in a track and the travelling distance of the testing rig is 50 m. Additionally, the rig has to be able to move to pre-determined distances, if it's input is to travel 2 meters then the rig has to move 2 meters. The accuracy must be within +- 5cm, relating this to the previous example, it should be able to travel in the range of 195 cm and 205cm.

On the last point, the manipulator chosen to hold the reflective metallic objects must be able to alternate the height up to 2m. For instance, if a robot arm is chosen that has a gripper to carry the test objects, the robot arm has to be able to lift the objects up to a maximum height of 2m meters. This also applies to it a platform is chosen as a design. The platform must be able to lifting mechanism that allows it to be lifted. Additionally, it must be able to lift to a specified height.

1.5 Thesis Contributions

The main contributions of this thesis are as follows:

- We propose a cost effective and accurate process to test radar technologies
- We have pioneered a new methodology using a unique technique which we conceptualised
- The design will be used to research the field more

1.6 Plan of development

The time given for the project is 13 weeks and the purpose of this section is to provide a breakdown of how the time will be managed to complete the project. The Gantt chart below provides a visual representation of the timeline.

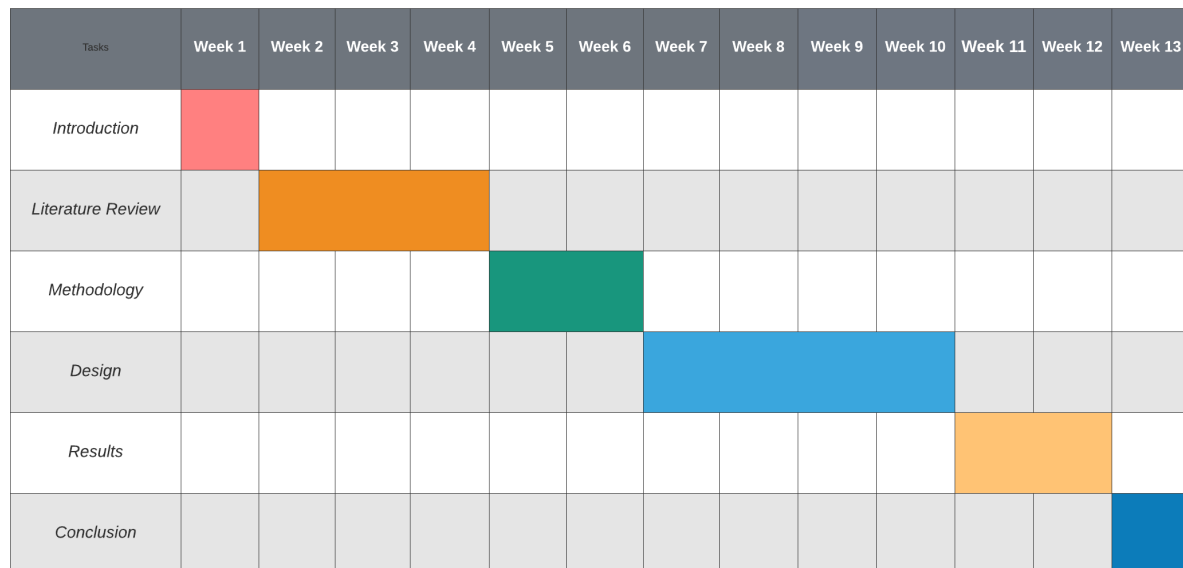


Figure 1.1: Gantt chart for the project

From figure 1.1 above it can be seen that the design section will be the section that the most time will be spent, this is because the design section has the implementation and testing embedded, there might be a possibility of multiple design revisions that might occur and therefore providing 5 weeks will be sufficient.

1.7 Scope and Limitations

The scope of the project is to design and build a radar test rig that is capable of traveling a desired distance and being able to lift test objects. The list below will describe in further detail of the scope and limitations.

- The time constraint is 13 weeks to complete the project and complete the thesis
- The budget for the entire project is R1500
- The test rig must be able to travel a distance with an accuracy of 5cm
- The test rig must be able to lift the test objects up to a height of 2m
- The test rig must be able to travel on asphalt or any flat surface,

The scope and the limitations of the project provide a rough guideline to the project. On the point of, lifting the test objects, the minimum height it should lift is 40cm, this will provide a basepoint to designing the final rig.

1.8 Thesis Outline

The remainder of this thesis is organized as follows:

Chapter 2, Background: Background and literature review

Chapter 3, Methodology: Project methodology

Chapter 4, Design: Design and development

Chapter 5, Results: Experimental results

Chapter 6, Conclusions: Conclusions and future work

Chapter 2

Literature Review

2.1 Literature Review

Steady and reliable motion of the built rig will be important to the success of the project. When testing radar systems, the testing environment has to be as stable as possible. This because radars are high precision machinery .This means the test rig has to be consistent, therefore many aspects of the project will be considered. The theory of the specific subject matter which is the design and build of a Low Radar Cross-Section Rig for Controlled Motion of a Calibrated Radar Target. This is a design orientated project therefore there is not much research that is done that pertains to this exact subject matter. Therefore, this literature review looks at a more granular perspective. Identifying different pieces that might be relevant to the project.

This chapter covers the theory needed for the project together with the necessary and relevant literature, and In the field of designing and building systems and machinery that can be moved accurately to predetermined positions, a myriad of applications

where predetermined movement is important. This has lead into research and development of various products and machinery. The objective of the literature review is to gain an insight into the various fields of research which involve controlled motion in different applications.

The first section of this literature review covers the needed theory of DC motors and the different types of DC motors, that will be relevant . Next the theory determining velocity and position using sensors, this theory will be salient in understanding the use of motors to move targets on a platform. Section 3 discusses different theories pertaining to different lifting mechanisms that will be connected to the research. Section 4 introduces a variety of different robots and machinery make use of the theory that was discussed in the previous sections. For each of the following areas of research that will be covered include velocity Estimation by Using Position and Acceleration Sensors, Point-to-Point Stable Motion Planning of Wheeled Mobile Robots.

2.2 Motor Theory

A motor is an electro-mechanical machine, it converts DC electrical power to mechanical power in terms of rotational energy using a direct current. The working principle of a DC motor is from The Lorenz force, which states that if a conductive wire loop is placed in a magnetic field, the moving current carrying electrons in the wire will interact with the magnetic field, and thus there will be a force acting on the wire [1] [2]. The equation of the force is as follows.

$$\vec{F} = \vec{I}L \times \vec{B} \quad (2.1)$$

Where:

- F is the resultant force
-

- I is the current flowing in the conducting wire
- B is the magnetic field
- L is the length of the conducting wire

The rotating part of the motor is known as the rotor. The rotor has the windings and the rotor core, that are excited by the DC supply. The stator is the stationary part of the motor and it contains the magnetic poles. The figure below illustrates a typical commercial DC motor [3].



Figure 2.1: Stator and Rotor of motor

2.2.1 Servo motor

The servo motor is an electrical device that rotates its shaft to precise angles. The servo motor has a DC motor embedded within the servo motor, along with the negative feedback control loop for detecting error and a gearbox. The [PWM](#) signal is used to control the servo motor and is applied to the spindle of the control signal. The servo control loop contains a comparator which compares the control signal (PWM) and generates the baseline signal from the potentiometer. The error signal is then magnified and sent to the DC engine. The DC motor shaft is connected to the potentiometer shaft (knob) by means of the gearwheel. Therefore, the direct current rotary motor rotates the potentiometer by changing the potentiometer reference signal provided to the comparator [4].

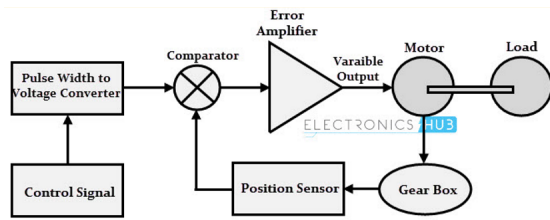


Figure 2.2: Block diagram of servo motor feedback

2.2.2 Stepper motor

A stepper motor is a type of DC motor that has an equal number of steps in each turn. It's a sort of actuator that works well with numerical control systems since it's essentially an electromechanical converter of digital impulses into proportionate shaft movement, allowing for exact speed, position, and direction control without the use of encoders. The frequency of input impulses can be changed to regulate the speed of a stepper motor over a wide range of values. For example, if the angular displacement per step is 1.5 degrees, the total number of impulses necessary for a complete revolution is 240, hence the motor's speed is 120 rpm at a frequency of 400 impulses per second [4].

2.2.3 BLDC motor

The Brushless Direct current motor(BLDC) is in actuality, a synchronous motor. The rotor follows a rotating magnetic field, and its motion synchronizes with the AC voltage applied to the winding. DC motor cooperates with the electronic drive controller to replace the function of the brush and convert the fed DC power into AC power, which achieve the performance equivalent to the brushed DC motor without the brush with limited service life. Therefore, BLDC motors are also called EC (electronic commutation) motors to distinguish them from mechanical commutation motors that include brushes. The BLDC motor is usually controlled by an ESC when

operated with a microcontroller [5].

2.3 Position and velocity sensing tools

2.3.1 Hall effect sensor

The hall effect is when a current carrying conductor is placed in a magnetic field, a voltage will be produced which is perpendicular to the current and magnetic field [6]:

$$V_H \propto \vec{I} \times \vec{B} \quad (2.2)$$

The hall effect sensor has a silicon piece embedded called the Hall element. The sensor produces a voltage when a magnetic field is present, which is the Hall voltage. The voltage output is a low level signal which is in the order of microvolts, for example 30microVolts for one gauss magnetic field detected. Therefore the hall element is connected to an internal differential amplifier

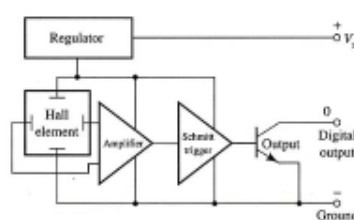


Figure 2.3: Internal circuitry of hall effect sensor

The Hall effect technology can be used to monitor and control the rotational velocity of motors. By sensing the change in magnetic field of the motor. Voltage pulses will be the output of the sensor , by connecting the hall effect sensor to a microcontroller, the necessary computations can be made to calculate the speed of the motor.

2.3.2 Tachometers

Tachometers are instruments that are used to determine the rotational velocity of a motor shaft of a disk. There are a variety of tachometers that are available. There are contact and non contact tachometers. The noncontact tachometers such as the optical/photo tachometers operate by shining an LED light or a laser beam at a rotating shaft or any rotating element. By shining this light source will have a reflection back off the shaft which is metallic or any reflective surface. The tachometer has an optical sensor internally, which is triggered as the reflected light shines back towards the sensor. By measuring the time it takes to get the light beam back to the sensor, the rotational velocity can be determined. The measurements units are Rotations Per Minute (RPM) [7].

2.3.3 Rotary encoder

Rotary encoders operate using similar methods, rotary encoders are found attached to electric motors. The encoder provides feedback in closed loop, therefore position and/ or speed can be tracked. There are a variety encoders and below is a list and a brief explanation of each encoder [7].

Servo Motor Encoder

Permanent magnet motor encoders, also known as servo motor encoders, are ideal for accurate and precise applications, as these offer a closed loop feedback control system. The accuracy and resolution can determine the encoder used, can be modular, incremental or absolute [7].

Stepper motor encoders

Stepper motors offer a more cost effective option, there is still accuracy and they are usually used in open loop configurations. These are used for applications that require open loop configurations. The stepper motor encoder are also able to run in a closed loop feedback configuration to allow for improved precision of the motor shaft or a disk in relation to the step angle [7].

The DC motor encoders are used to control speed of the DC motor shaft in closed loop.

2.4 Robots with lifting mechanisms

2.4.1 Predetermined motion planning for wheeled robots with arms for object

Alipour and et al study into point-to-point stable motion planning of wheeled mobile robots with multiple arms for heavy object manipulation provided important information about autonomous robots that have manipulators/arms to carry large objects. Autonomous wheeled mobile robots (WMR) that are equipped with manipulators, combine the locomotion abilities and their dexterous manipulation. The robot poses new challenges in terms of designing, control and planning the route of the robot. While carrying a heavy payload, the robot will have to maintain correct posture to remain balanced. This means that the initial and final positions of the payload will have to be specified. After specifying the initial and final positions of the arm position of the payload, the trajectory of the robotic arms relative to the moving base are planned to ensure the stability of the robot through the planned trajectory or route of the robot. The problem of stability is solved as an optimization problem. An appropriate cost function is formulated and implemented, which

is to be minimized. The WMR that is equipped with two 3-Degrees Of Freedom manipulators as shown in the figure below [8].

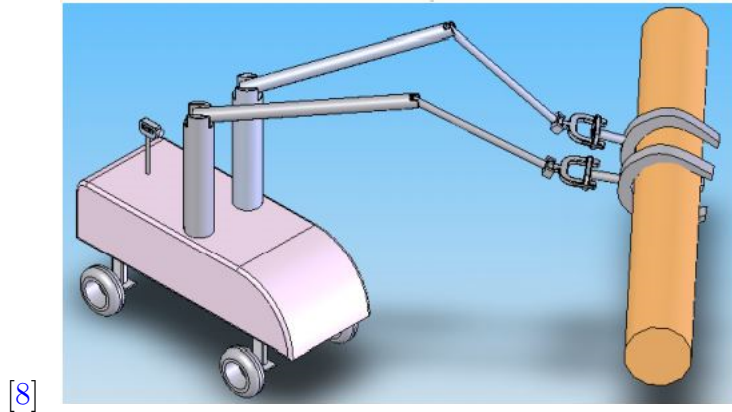


Figure 2.4: Autonomous WMR

The main goal of the paper was to be able plan the motion of the wheeled robots while manipulating a heavy payload from an initial pose to a predetermined final one with the balance of the robot and the postural stability of the system is maintained. The arms carrying the payload exert longitudinal tractive force lateral force and heading angle torque on the platform. To make sure that the system is stable throughout the entire path. The inverse kinematics of the end-effectors with respect to the platform, from there, the line of steepest descent algorithm is used to determine the optimal path to be taken to ensure stability. In conclusion, in order to keep the entire system in dynamic equilibrium during the heavy object manipulation task. The important point from this particular paper is that the stability of wheeled robots is salient and the path of the robots are to be planned thoroughly, with high accuracy. These points are of importance in this research .

2.4.2 Hybrid Serial-Parallel Mobile Robot

In the following study, Moosavian and Hoseyni set out to investigate the dynamics and stability of a novel serial-parallel wheeled robot. What makes the robot novel is that the manipulator which is attached to the base of the robot, is able to move the arm spatially to maintain the stability of the robot in uneven terrains with unknown obstacles and disturbances whilst carrying heavy loads. The spatial parallel mechanism has 3DOF, it uses three planar actuators which are arranged in a prismatic configuration. The end-effector has no degrees of freedom, therefore the translational motion relative to the base is the mechanism that allows maneuverability of the arm. Stable motion is a reoccurring problem that is faced in motion of wheeled robots which have manipulator arms. In order for the system to be stable the center-of-mass of the entire system must be relatively low. This brings the other advantage of the spatial parallel system, the mechanism is able to alter the robot's center of mass by adjusting its height, this structure is thus named the hybrid serial-parallel robotic system. This suggested structure combines the advantages of both serial and parallel robots, this is achieved by moving the base point of the serial robot with respect to the wheeled platform. The figure of the robot is shown below [9].

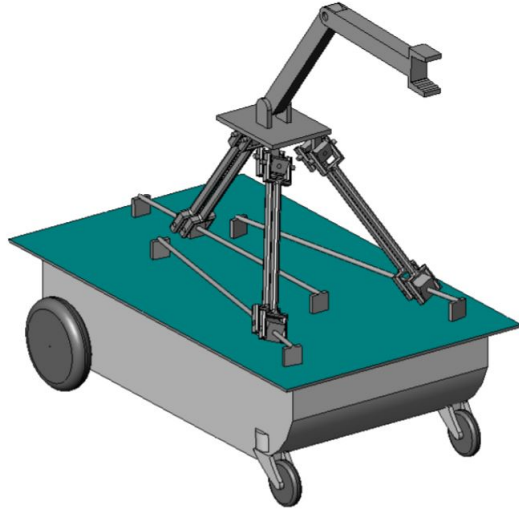


Figure 2.5: the model of the robot
[9]

The advantages of a spatial parallel mechanisms are:

- A low weight/load ratio
- High rigidity
- High accuracy
- A localized workspace

The upper plate of the spatial parallel mechanism only moves in the cartesian space as a consequence of having only parallel actuators. When we modeling the kinematics and dynamics of the system, the constraints and DOFs were first stated. The system uses a differentially driven wheeled base, which has a nonholonomic constraint. Nonholonomic means it can be made independent of velocities therefore it does not reduce the generalised coordinates in configuration space. The parallel system has six holonomic constraints [10]. These holonomic constraints restrain the upper plate from rotating , and the nonholonomic constraint , eliminated the wheeled

base sliding along the axle of the wheels. The Moment Height Stability measure of the which was calculated by the forces and torques that are acting on the base of the robot, this stability was increased by using the parallel mechanism. In the end of the research it was conclude that having the system greatly improved the mobility and stability of the robot when traversing and manoeuvring heavy objects, the optimal control method was key in stabilising the system. The limitations of the carrying capacity was the limits of the actuators and the end-effector.

2.5 Possible Control methods

A closed-loop control system is a type of control system in which the controlling action shows dependency on the generated output of the of the system. The variation input which is dictated by the output leads to producing a more accurate system output. Closed-loop systems are considered as fully automatic control system because it is designed such that the desired output is automatically without having to adjust the setpoint. Relying on the feedback and controller to guide the plant to desired performance. In terms of the type of closed loop controllers, there is myriad of control types that can be used. They all differ in performance, implementation and computation. For this section, the research will be limited to controllers that will be relevant to this particular project. Which will be PID and Sliding mode controllers. The reason being the controllers meet all of the requirements, in terms of performance [11].

2.5.1 PID Control

A PID is a combination control actions namely proportional, integral and derivative, hence the name PID (Proportional-Integral-Derivative) controller. These three control actions are varied for specific application to obtain the most optimal response

from the plant. The input of the PID controller is the desire output being subtracted by the actual output, which is referred to as the error. Each of the three control actions have their own purposes. Proportional controller produces the control output which is proportional to the error. The error value is scaled or multiplied by (K_c) which is the proportional gain, the gained error determines the output response. The integral controller is important because it reduces the steady state error of the system. The integral accumulates the error terms over a period of time until the error reaches zero. As a result, even small error causes a substantially high integral control motion, it holds the previous output values in order to maintain the zero steady state error. A derivative controller monitors the speed in which a variable changes per unit time, and produces an output which is proportional to the rate of change. The derivative controller is important when the variables in the plant have a higher rate of change [12].

The paper published by V. V. Khulkami used a PID controller to control the rotational velocity of a DC motor. The motor was modelled and controlled in MATLAB and the control law was implemented using the Arduino development board, the results showed that the PID is adequate for controlling DC motors [13]. There was no overshoot on the speed and the motor is able to avoid input and output disturbance. PID control is very versatile and can be used in most situational that need a control law to execute. The paper released by A. Iyer et al which modelled simulated and implementation of a PID controller on quadrotors. A quad-rotor is a type of Unmanned Aerial Vehicle (UAV). UAVs fall under the category of drones. Quad-rotors are nonlinear plants therefore implementing control systems can be very challenging. The outcomes of the paper is that the PID algorithm that is found is good enough to elicit the desired response from the drone [14].

2.5.2 Sliding Mode control

Sliding mode control(SMC) is a nonlinear control technique featuring remarkable properties of accuracy, robustness and easy tuning, lastly it is easy to implement. SMC systems are designed to drive the systems states onto a particular surface in the state space, this space is named the sliding surface. Once the system's states have reached the sliding surface, the sliding mode control keeps the states on the close vicinity of the sliding surface [15]. The sliding mode control is a two part design. The first part involves designing the sliding surface so that the sliding motion satisfies the design specifications. The second part of the task is selecting the control law that will make the sliding surface more accessible to the system state.

The sliding mode control law is often used as the preferred control approach because it is efficient and robust. This control law is most effective when dealing with complex high-order nonlinear dynamic models which are operating under uncertain conditions. One of the major advantages that sliding mode control has is low sensitivity to plant parameter variations and disturbances. This point is of importance because, it eliminates the necessity of modelling the plant exact. Sliding mode allows the fragmentation of the overall system into independent partial components that are lower dimensions and as a consequence, drastically reduces the complexity of the feedback control design. Sliding mode control has been proven to be applicable to a myriad of problems in electric drives, generators , process control, robotics, vehicle and motion control.

A paper wrote by P. Ghalimath et al, used the theory of Sliding mode control to control the velocity of the DC motor, the SMC performance was compared to the performance of the PID. It was found that the sliding mode approach had smoother control action. In the case of output disturbances , the sliding mode gives the best

disturbance rejection in the experiments ran in the project. This can also be said about input disturbances. And finally, when there are time delays, the sliding mode control is the better approach in this particular study. The sliding mode control proves significantly effective in a variety of motors [16]. A paper released by E. Quintero-Manríquez et al investigated the use of a second-order sliding mode speed controller, along with anti-windup and the super-twisting algorithm, for Brush-less DC motors(BLDC). The results of that paper displayed that the performance of the motor was greatly improved by using SMC. The anti-windup improved performance when the manipulated variables are saturated , most of the performance gains is a result of the SMC.

Chapter 3

Methodology

This chapter This section aims to detail the processes and methods that will be followed in order to solve the engineering problem at hand.

3.1 Problem identification

The Design, Development and Implementation of an affordable low radar cross-section rig which meets the requirements. The literature review chapter provided readings and research that might be of use in this particular research project. Using some of the theory that was in the literature review can be a framework which the project can operate under. The project will be using a V-model of development which will be discussed further in this chapter, but first the requirements of the project must be formulated and analysed before moving on into any of the design aspects of the project. The chapters that proceed will divulge more into the design and implementation, along with the results obtained from the implementation and finally the conclusion which will discuss the results and provide any further recommendations to the project.

3.2 System Requirements

From the problem identification section the requirements of the project can be formulated and analysed, following that there are verification stages that will validate if the requirements have been met.

The following table shows the system requirements for the system. The requirement Identification used is **S.R** and the numbering starts at 001.

Table 3.1: Table of System Requirements

Req. ID	Requirement Text
S.R.001	The system has to be able to handle the lightweight objects without damaging them.
S.R.002	The rig should be able to travel a specified distance
S.R.003	Should be able to adjust the rig's height.
S.R.004	Has to be lightweight
S.R.005	The system should have a separate power supply

3.3 Requirement analysis

The following tables are functional requirements derived from system requirements and the Requirements Identification is **F.R** and the numbering starts from 001.

3.3.1 Analysis of S.R.001

"The system has to be able to handle the lightweight objects without damaging them."

Whilst the rig is handling the test objects (which are the metallic objects used to

test radar), the rig must not cause any damage to the objects in the entirety of its testing.

Table 3.2: Functional Requirements table

Req. ID	Requirement Text	Derived From
F.R.001	The materials used to construct the rig must be rigid	S.R.001
F.R.002	The rig must be an enclosure for the test objects	S.R.001

From the requirements of the system requirement quoted above, the table 3.2 is the requirements the rig's structure that must be met.

3.3.2 Analysis of S.R.002

"The rig should be able to travel a specified distance"

The system should have the functionality of being mobile, motorised and should have a method of measuring the distance travelled.

Table 3.3: Functional requirements from S.R.002

Req. ID	Requirement Text	Derived From
F.R.003	The rig should be driven by a motor system	S.R.002
F.R.004	There should be a microcontroller to control the motor system	S.R.002
F.R.005	The speed should be able to be measured and controlled	S.R.002
F.R.006	The distance covered by the rig should be able to be measured and controlled	S.R.002

3.3.3 Analysis of S.R.003

"Should be able to adjust the rig's height."

The objects that the rig is handling should be able to be hoisted in a range of heights which are in the scope of the project.

Table 3.4: Functional requirements from S.R.003

Req. ID	Requirement Text	Derived From
F.R.007	There should be a lifting mechanism	S.R.003
F.R.008	The lifting mechanism should be variably height adjustable	S.R.003
F.R.009	The lifting system should be able to lift to a height of at least 40 cm	S.R.003
F.R.010	The lifting mechanism should keep the testing objects level	S.R.003

3.3.4 Analysis of S.R.004

"S.R.004 Has to be lightweight"

The rig has to be portable for it to be able to operate in different places, therefore the rig itself must be light enough to be somewhat portable.

Table 3.5: Functional requirements from S.R.004

Req. ID	Requirement Text	Derived From
F.R.011	The entire rig must weigh less than 10Kg	S.R.004
F.R.012	The material used to construct the rig has to be light e.g(3D printed, aluminum, etc)	S.R.004

3.3.5 Analysis of S.R.005

"S.R.005 The system should have a separate power supply"

The testing rig should have a DC Power Source such as a battery that will allow it to operate independently.

Table 3.6: Functional requirements from S.R.005

Req. ID	Requirement Text	Derived From
F.R.012	A Battery that will power the electronics of the rig	S.R.005
F.R.013	The battery must be able to fit inside the form factor of the rig	S.R.005

3.4 Verification

The verification stage is the point in which the functional requirements are verified by validating the outputs of the system with the functional requirements set out in the previous subsection. The verification identifiers will be classified as **R.V** and the numbering begins from 001. These verification steps can also be viewed as Acceptance test procedures,

Table 3.7: Verification table

Ver. ID	Verification	Derived From
R.V.001	The requirements will be verified by testing the loading strength of the rig and its ability to carry the test objects, used in testing radar	Requirement Analysis of (S.R.001)
R.V.002	The requirements will be verified by the ability of the rig to traverse the track without stopping until it has reached the required distance. The speed of the rig should also be able to be measured and adjusted if need be.	Requirement Analysis of (S.R.002)
R.V.003	The requirements will be verified by the rig's capability of lifting the objects to a specified height and maintaining the height throughout the track	Requirement Analysis of (S.R.003)
R.V.004	The requirements will be verified by weighing the weight of the components and see if they cumulatively weigh 10Kg or less.	Requirement Analysis of (S.R.004)
R.V.005	These requirements will be verified by checking if the rig can operate without the use of any of the lab's power supplies. Be powered only by the battery pack.	Requirement Analysis of (S.R.005)

The table 3.7 explains the possible verification and validations steps that might be taken to make sure that the functional requirements may be able to be met

3.5 Design Process

In order to execute all of the requirements and deliverables of the project, a Model Based System has to be implemented. Model-based systems engineering is the formalized application of modelling to support system requirements, design, analysis, verification and validation activities beginning in the conceptual design phase and continuing throughout development and later life cycles. There are several design models which are all use different development models to solve the engineering problem.

3.5.1 V-model Design process

The design process that will be used in this project is the V-model approach. a V-model approach is one in process which is highly structured, where there is a testing phase which is parallel to each developmental phase and it follows a sequential approach. The reason for the choice of model is that Testing happens well before implementation, which to higher chance of success. And errors can be detected earlier.

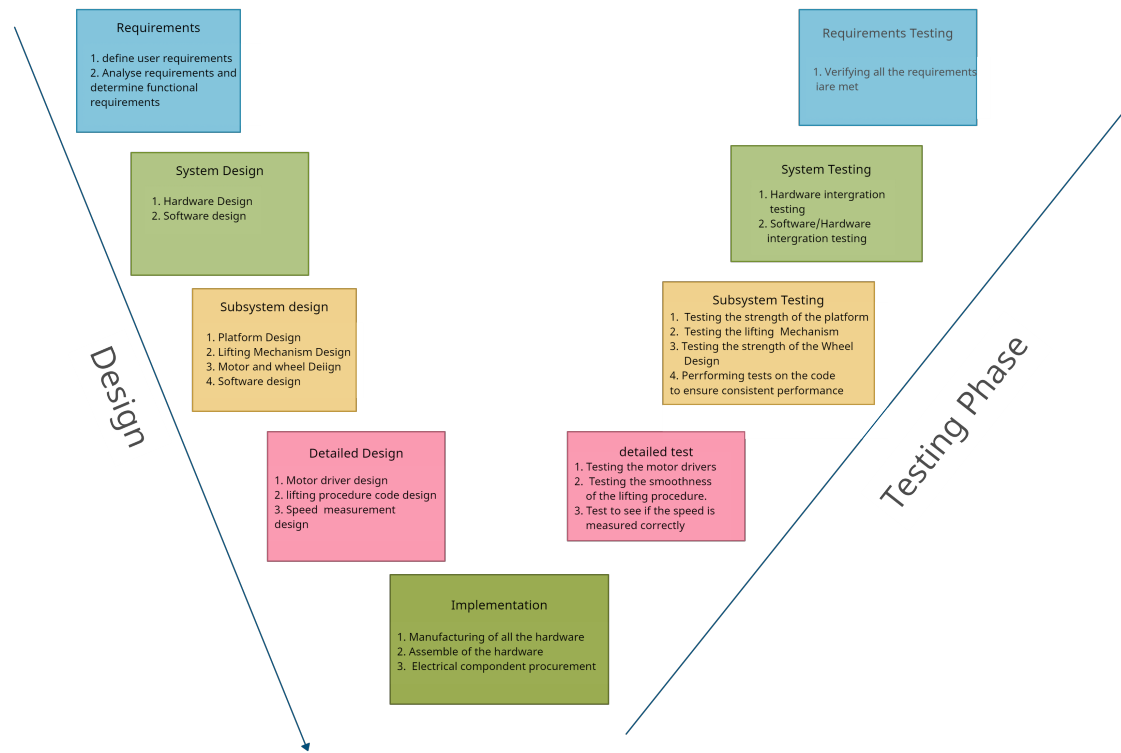


Figure 3.1: V-model of the project

The figure above 3.1 is a V-model diagram which explains the methodology and the design process that will be followed in the project.

;

;

Chapter 4

Design

The design chapter will cover all sections of the projects in depth in terms of design choices, process of designing and implementing the different subsections of the process Using 3 as a guideline. This is because the methodology contained guidelines to the majority of the design decisions that will be used in this chapter.

The first subsection will contain the overall system design and how the rig will operate. Then the hardware of the system will be explained in detail. In terms of components chosen, manufacturing and how the hardware integrates to work in unison with one another. From there the software design of the rig will be discussed, how the different software subsections come together to work cohesively.

Lastly, the physical implementation of the rig will be shown and how all of the software and hardware integrate to the final output of the system. This physical implementation is a physical realisation for all the design decisions taken in the previous subsections.

4.1 System Design

This section covers the overall system design of the test rig. This is a very high level abstraction of all of the subsystems and how they interact with one another. Additionally, it shows how the user will be interacting with the entire system.

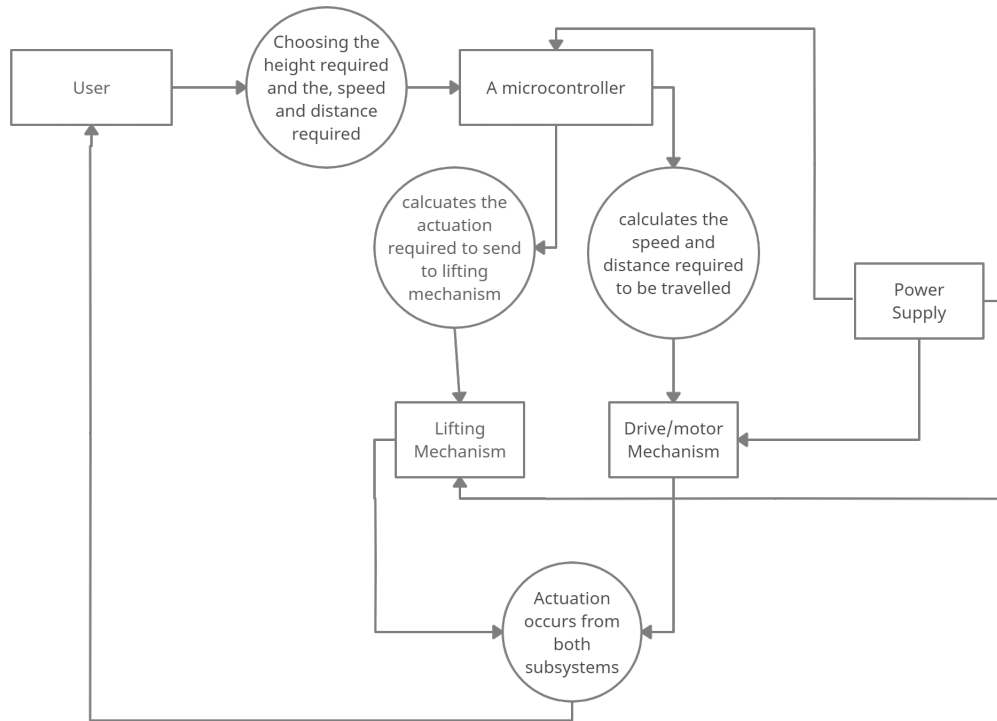


Figure 4.1: OPM Diagram of the basic operation of the rig

The figure 4.1 shows the basic working of the rig. When the rig is assembled, the user has to input the height that the needs to be and the distance the rig has to follow and the speed. For the first implementation it will be 5 different modes, 1 being the lowest speed and 5 being the highest speed. The second implementation which may be beyond the scope is inputting a specific speed. After inputting the speed and height, the rig will send those commands to the microcontroller such that the it is able to perform the calculations that are needed to lift the platform and travel the

distance specified and then that is sent to the lifting and motorised mechanism and finally the rig moves as required so that the user can test the radar using this rig.

4.2 Hardware Design

In this section all hardware related aspects of the rig will be discussed, from the design of the rig to components chosen. Following this, modeling, data collection and testing is performed on all of the hardware.

4.2.1 Components Chosen

Feetech 360 Servo

This FS5113R Feettech Servo is a continuous rotation standard servomotor which has a 360° operating angle with metal gears. The operating voltage range is 4.8-6 volts with a stall torque of 14kg.cm at 6V. The Wire length is 30cm, this servo motor will be used for the lifting mechanism that will be discussed in the following chapters. The reason why I chose this servo motor was because the torque it provides is enough for this particular application and the dimensions of the servo are perfect. Some of the specs of the servo are listed below:

- Operating Speed: 0.18sec/60degree (4.8V) ,0.16sec/60degree (6V)
 - Stall Torque: 12.5kg.cm (4.8v) , 14kg.cm(6V)
 - Operating Voltage: 4.8V 6V
 - Control System: Analog
 - Operating Angle: 360 degree
 - Required Pulse: 500us - 2500us
-

- Dimensions: $40.8 \times 20.1 \times 38$ mm

The image below illustrates the servo motor and its dimensions:

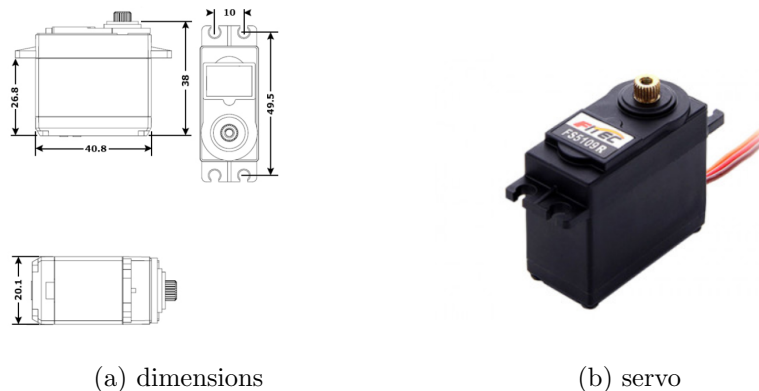


Figure 4.2: The servo motor with the dimensions

Arduino UNO R3 - Original

The arduino uno r3 is going to be used as an interface to communicate with all of the components of the rig and perform all of the computations in terms of mobility of the test rig. This particular arduino was chosen because there are a great number of GPIO pins and PWM pins that will be useful. The list below is some of the specifications of the arduino:

- ATmega328 microcontroller
 - Input voltage - 7-12V
 - 14 Digital I/O Pins (6 PWM outputs)
 - 6 Analog Inputs
 - 32k Flash Memory

- 16Mhz Clock Speed

The figure below shows the schematic of the arduino and the board.

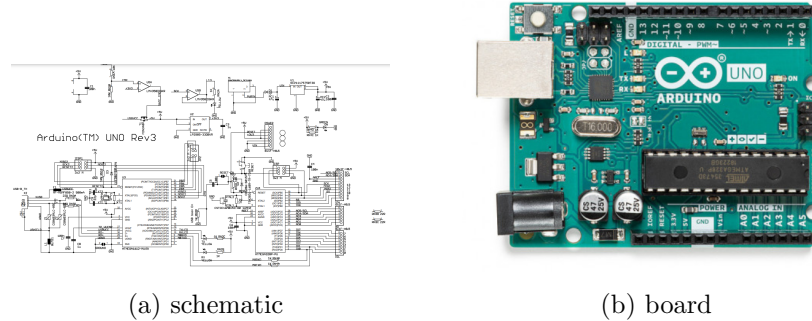


Figure 4.3: The arduino UNO R3 and schematic

HKD 795 Motor

The HKD 795 Motor is a high power motor and this motor will be used to enable mobility for the rig. There will be 2 of these motors which will be used to move the entire rig. The motor has high torque which is needed for moving this rig because of the weight and size. Some of the specifications of the motor are listed below.

- Voltage DC 12V-24V
- Load AMPS 2.05A
- Load speed 12V(10 000rpm) - 24V(20 000rpm)



Figure 4.4: DC motor
Akhile Ngwenya - Electrical Engineering

As it can be seen above 4.4 shows the motor and the dimensions of the motor.

HKD Speed Sensor

The speed sensor is used as a rotary encoder that is used to calculate the speed of DC motor using pulse detection. This particular sensor was chosen because of the range of operating voltages and it is an important sensor because it will be used to estimate and control the angular velocity of the HKD 795 Motor.



Figure 4.5: Encoder

The rotary encoder above 4.5 is an optical encoder which can interface with a microcontroller to interpret the information.

L298 Dual H-Bridge Motor Driver

This module is based on the very popular L298 Dual H-Bridge Motor Driver Integrated Circuit. The circuit will allow for to easy and independently control two motors of up to 2A each in both directions. It is ideal for robotic applications and well suited for connection to a microcontroller requiring just a couple of control lines per motor. Therefore this module was needed for rig, because the Arduino needs to communicate with the motors and this module provides an interface to control up to 2 motors. The list below is some of the specifications:

- Motor supply: 7 to 24 VDC
- Output Power: Up to 2A each

- Enable and Direction Control Pins

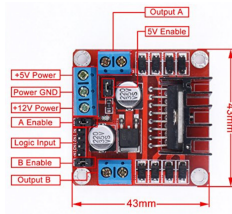


Figure 4.6: Motor Driver

As it can be seen above, 4.6 illustrates the pin layout of the driver, such as the enable jumpers for the two motors and the pins used to interface with the micronotoller.

RT1265 12V Battery

The battery will serve as a power source that will be in charge of powering the DC motors. The dimensions of the battery were key in choosing the battery.

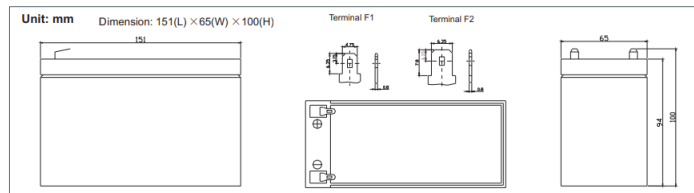


Figure 4.7: 12V battery

The dimensions of the battery are illustrated in 4.7

4.2.2 External Rig Design

??

The design of this shell should be built to meet all of the system and functional requirements discussed in 3, therefore overall design should be based around the strength and stability of the rig. The following subsections discuss different parts of the external design.

Design of platforms

Firstly, the lower platform will be discussed. The lower platform is responsible for several points in the whole rig.

- It behaves as a chassis for the wheels
- It houses the electronics
- It holds the lifting mechanism
- It supports the upper platform

Therefore the dimensions of the platform should be able to perform all of the tasks listed above. The following 3D model is the design of the platform.

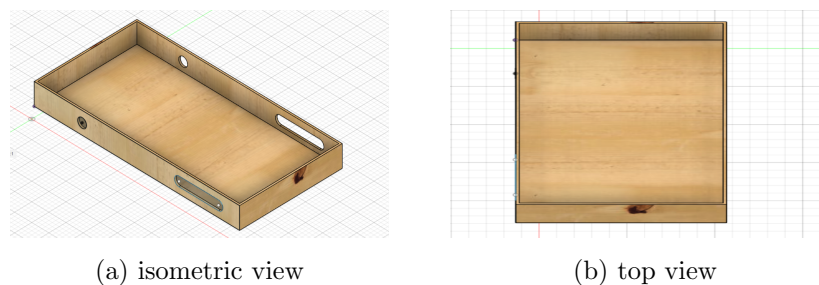


Figure 4.8: The isometric and top view of the lower platform

The length is 600mm, the width is 300mm and the height is 60mm. The following figure shows the profile of lower platform.

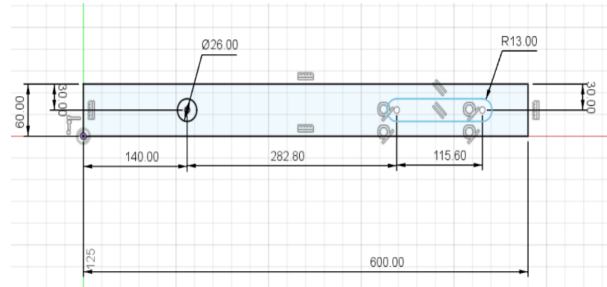


Figure 4.9: Lower Platform profile

The upper platform is in charge of holding the test objects. The upper platform is 100mm shorter in length compared to the lower platform, but the width and height remain the same. The distance between the 26mm diameter hole and the 115.6 mm long slot. The holes that are seen in 4.9 are going to have pvc pipes through them and they will be holding the lifting mechanism.

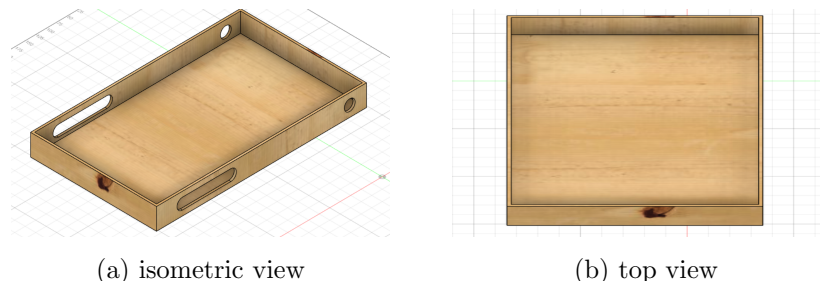


Figure 4.10: The isometric and top view of the upper platform

The following figure illustrates the profile of the upper platform.

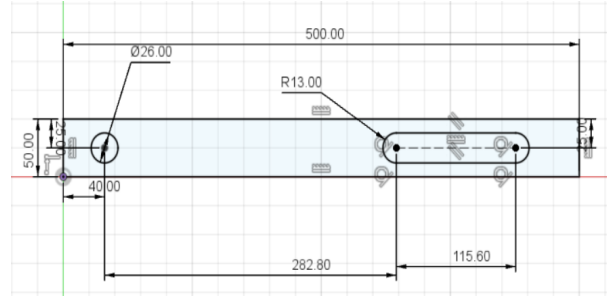


Figure 4.11: Upper Platform profile

The design decisions for the dimensions will be discussed further in the following subsection.

Design of lifting Mechanism

For this section of the design, a scissor lifting mechanism is chosen in order to lift the test objects and upper platform 500+ mm. The scissor lift will be assembled by 4 arms on each side. The following figure is one of the arms.

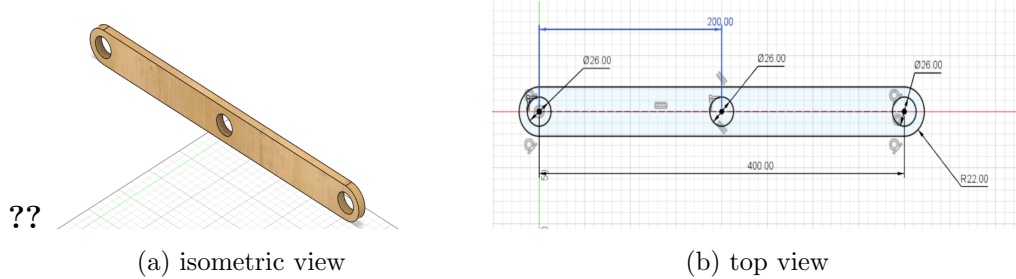


Figure 4.12: The isometric and profile view of the lifting arm

The scissor lift mechanism will be able to suspend the test objects up to a height of 560mm. this is achieved by having the 4 interlocking arms perpendicular to one another in the following arrangement:

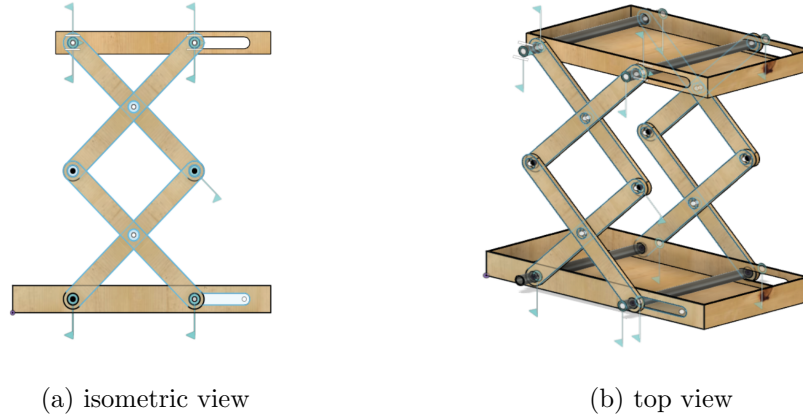


Figure 4.13: The isometric and profile view of the lifting mechanisms

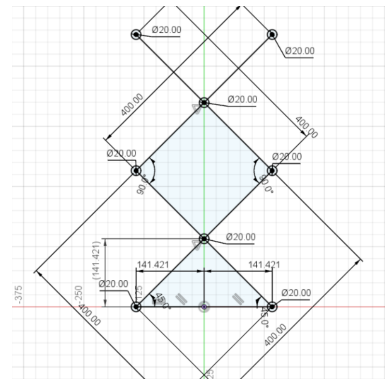


Figure 4.14: Diagram of the dimensions of the lifting platform

From 4.12, it can be seen that the length of the slots is 400mm and the figure 4.13 illustrates how the slots will be arranged the 26mm hole cutouts will serve as hinge points with 25mm diameter PVC pipes that serve as shafts. The lifting arrangement in 4.15 illustrates how high the upper platform will be suspended. The slots are at a 45° with the lower platform. Half of the slot length is 200mm which is a hypotenuse of the right angled isosceles triangle and using trigonometry, we can get the vertical height.

$$height = 200 \sin 45 = 100\sqrt{2} = 141.4213mm \quad (4.1)$$

Therefore the total height is $4 \times 141.4213\text{mm}$ which is 565.6854mm . The lowest the platform can be folded is when the links are fully extended to the end of the slot in [4.13](#) and the scissor lift arrangement is illustrated below.

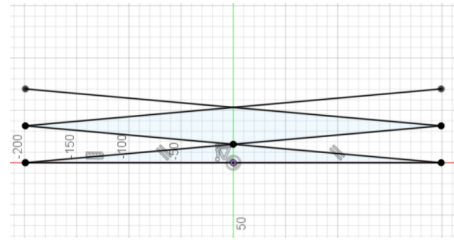


Figure 4.15: Diagram the scissor lift in its lowest height setting

Using the equation [4.1](#), additionally the slot makes a 5.05° slope to the horizontal, it can be seen that the vertical height is 17.705mm , therefore the total vertical height is 70.42mm .

Pulley system

The scissor lift mechanism will need the servo to pull the PVC pipe in the slot, and that is where the servo will be useful the servo will pull the pipe. The servo will work in a pulley system where there will be a cable or rope pulling on the lifting mechanism. The design of the pulley is below:

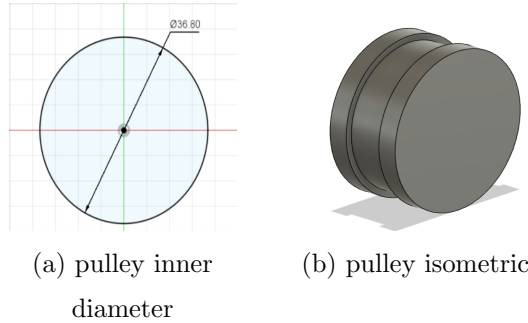


Figure 4.16: The isometric and profile view of the Pulley system

The inner diameter of the pulley is 36.8 mm wide, which is a circumference of 86.8π which is approximately 270mm, which is the same as the length of the slot in figure 4.8 which means that the pulley will make one full rotation to traverse the entire slot to lift the scissor platform. The pulley will be powered by the servo motor and the servo needs a housing which is below.

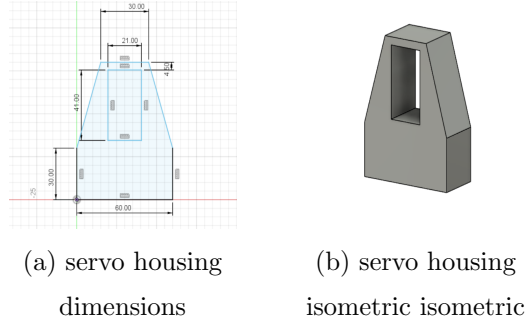


Figure 4.17: The isometric and profile view of the servo motor housing

As it can be seen from figure ?? the cavity is the dimensions of the servo motor.

Back Wheel Design

The figure below illustrates the housing of the DC motors that drive the backwheels.

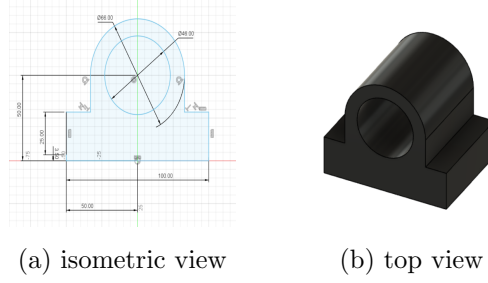


Figure 4.18: The isometric and profile view of the Motor holder

The dimensions of the cavity in 4.18 is the width of the DC Motor that will drive the wheels. The overall height of the housing is 73mm, this is to give enough clearance for the lower platform, additionally the length of the housing is 75mm.

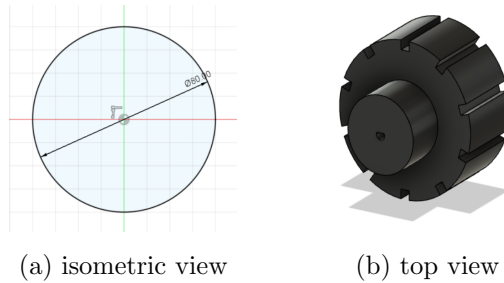


Figure 4.19: The isometric and profile view of the Back Wheel design

The diameter of the back wheels in 4.19 is 80mm and the width is 40mm, additionally there is a 25mm tall stem that connects the back wheels to the DC motor. There are 5mm deep grooves of the wheel to increase traction with the ground.

Front wheel design

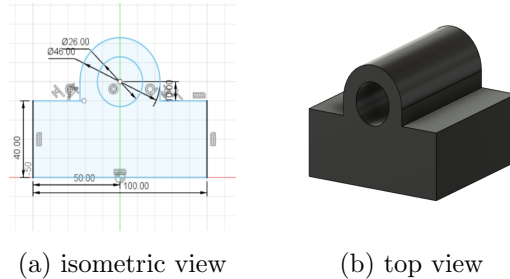


Figure 4.20: The isometric and profile view of front wheel shaft housing

The front wheel shaft housing is the support structure for the front wheels. The 26mm diameter hole in 5.12 is for a PVC to act as a shaft that will support the front wheels. The total height of the housing is 63mm, This is to match the clearance of the back wheels to ensure that the bottom platform is level.

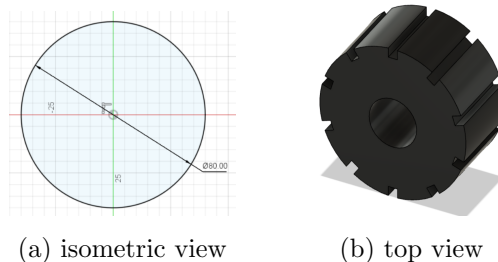


Figure 4.21: The isometric and profile view of the Front Wheel design

Looking at the dimensions of the front wheel in 4.21, it can be seen that it possesses the same grooves as the back wheels the differences are that the front wheels have a 26mm diameter pocket which the PVC pipe will go through the pocket.

The next section will talk about the electronics of the rig and how they interact with one another.

4.2.3 Electrical Component layout design

Motor drive Circuit

This subsection describes how the motors are driven by the arduino and how the encoder is used to measure the rotational speed of the rotor. The figure below illustrates the electrical connections to the different components.

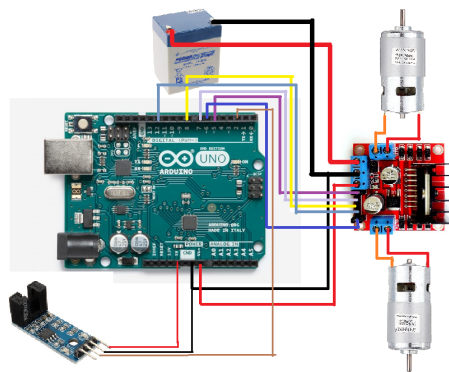


Figure 4.22: Diagram of the electrical connections of the Motor Drive system

The [4.22](#) is a visual representation of how the wiring of the drive system. The table [A.1](#) found in APPENDIX A, describes how the Arduino is connected to the Motor Driver, how the motors are connected to the driver, additionally, how the optical rotary encoder is connected to the arduino,

The first motor is connected to the OUT 1 and OUT 2 pin of the motor driver, these pins feed the output signal which drives the Motors clockwise or counter-clockwise. The ENA pin from the driver receives a PWM signal from pin 5 of the arduino, This PWM signal is integral in running the motors. The GPIO pins 7 and 8 are connected

to IN 1 and IN 2 of the driver. Setting Pin 7 to be High and pin 8 to be low will drive the motor clockwise and when set vice-versa, the mototr will rotate counter-clockwise. The same logic is applied to the second motor and the corresponding connections. The motors are powered by a 12V 5AH battery.

The optical rotary encoder will be key in measuring the rotational velocity of the motors. The diagram in Figure 4.5 shows that the encoder has a slot, which houses a transmissive optical sensor with phototransistor output. When the slot is not blocked thre D0 pin is active low, until athe slot is covered, then there will be a digital High signal sent to D0 which is connected to Pin 2 of the arduino. Pin2 is set as an interrupt, The interrupt will be elaborated further in the Software Design section

The rotary encoder is mounted on the side of the motor housing to interact with A 3D printed part which is the slotted disk shown below.



Figure 4.23: Diagram of the Slotted disk

Figure 4.23 is the disk that will be attached to one of the back wheels as they rotate. The encoder and disk will be in the following configuration.

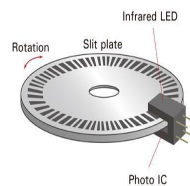


Figure 4.24: Diagram of the Encoder-Disk configuration

Akhile Ngwenya - Electrical Engineering

As the wheel turn, disk spins at the same speed and the slots pass through the gap of the encoder, sending high pulses every time the gap is blocked, using these pulses and some calculations which will be performed by the arduino, the code for this section will be discussed in the Software design section.

Electronics for Lifting Mechanism design

The figure below is the pin connections for the servo motor and the arduino.

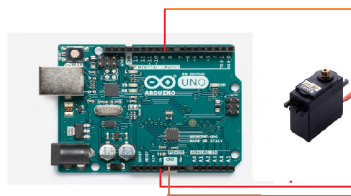


Figure 4.25: Diagram of electrical connections for Lifting mechanism

Figure 4.25 illustrates how the servo receives the PWM signal from the arduino, the table A.1 contains the pins that the servo is connected to. Pin 9 is connected to the signal pin of the servo motor and VCC is connected to the 5V pin and the GND pin is connected to he ground pin of the arduino. The PWM signal alters the angle of rotation from 0° to 360° continuously. The software design section will discuss how the scissor lift mechanism interacts with the arduino and the calculations performed.

4.3 Software Design

In this section, the algorithms that are used to measure the speed of the motor and determine distance travelled by the motor will be discussed, additionally the calculations and operations used to determine the how high the lifting platform has to be lifted will follow. The flowchart below is an overview of the algorithm that the

rig will follow in order to meet the requirements, each section of the flowchart will be explained in greater detail in the following subsections.

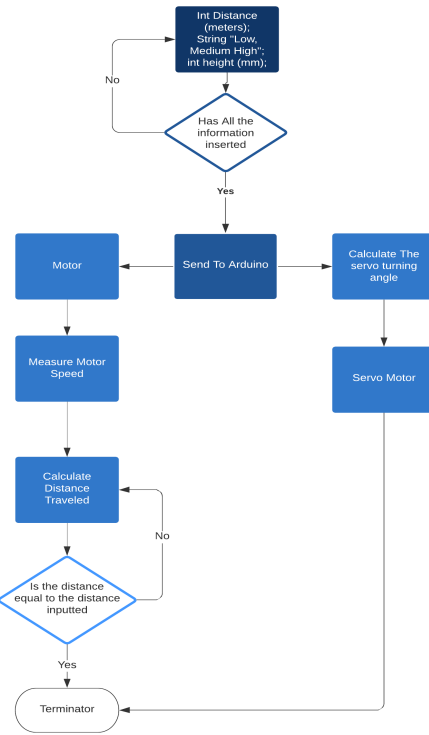


Figure 4.26: Flowchart of the software design

The figure 4.26 is an abstracted view of the different operations occurring to move the rig and the lifting mechanism actuator. The user inputs the desired distance to be travelled by rig, secondly, the desired speed of the rig and lastly, the height in which the rig has to lift the test objects.

4.3.1 Motor Drive System

The following subsections will explain in detail, the different parts of the code that operate together to make the entire system run.

Measuring rotational speed of the motor

The rotational speed is going to be measured using the encoder and the slotted disk in the configuration used in figure 4.24. The pin connection and how the encoder is going to interact with the arduino was explained in subsection 4.2.3.

The pins are being setup in A.3. Within the setup code, it can be seen that the D0 pin of the encoder is connected to one of 2 interrupts, which is in pin 2. The code below is a method which has an incremental counter which increases as soon as an interrupt is detected by the arduino.

```
1 void ISR_count1()
2 {counter1++;}
```

This is called an Interrupt Service Routine, the counter variable will be used to calculate the speed. The following code is how the calculations are performed.

```
1 void ISR_timerone()
2 {
3     Timer1.detachInterrupt(); //stops the timer
4     Serial.print("Motor_Speed");
5     float rotation1 = (counter1 / diskslots)*60.00; //
6         calculate
7     Serial.print(rotation1);
8     Serial.println("");
9     counter1=0; // reset counter to zero
10    Timer1.attachInterrupt( ISR_timerone ); //Enable the
11        timer}
```

Since there are 15 slots of the disk, the number of interreupts counted in the rotation have to be divided by 15 to obtain the rotational velocity of the motor in rad/s.

Multiplying by 60 gives the number of rotations per minute (RPM), and the this data be be uploaded to the serial monitor to be used as data in the later subsections. The ISR_timerone() method calculates the speed every 100ms which can be seen in the setup code in [A.3](#).

Issues with measuring the rotational velocity

The rotary encoder seems to have physical limits in terms of maximum sampling frequency. because when the motor was tested, the encoder stopped sampling at a certain speed, this happened when the 15 slot disk was used to measure the speed. The internal circuitry of the encoder can be found in [A.1](#). Therefere, it was decided 1 slot will be used instead to prevent aliasing. The consequence of this though will cause the data to lose its precision

Modelling a motor

There are a myriad methods to model a brushed DC motor such as the one that was chosen. The circuit diagram in [A.4](#) will give us a bases to begin mathematical modelling of the system.

The equation below is a general equation that governs the dynamics of a DC motor:

$$R_a i_a(t) + L_a \frac{di_a(t)}{dt} + v_b(t) = v_s(t) \quad (4.2)$$

Where:

R_a is the armature resistance

$i_a(t)$ is the armature current

L_a is the armature inductance

$v_b(t)$ is the back EMF of the the motor

$v_s(t)$ is the supply voltage

The back EMF voltage of the motor is proportional to the angular velocity with the following equation.

$$v_b(t) = k_b \frac{d\theta(t)}{dt} \quad (4.3)$$

Where k_b is the constant of back EMF. The motor generates torque when rotating which is proportional to the armature current as shown below.

$$T_M = k_T i_a(t) \quad (4.4)$$

Where T_M is The generated torque, and k_T is the torque constant.

Substituting equation 4.3 into 4.2 we get:

$$R_a i_a(t) + L_a \frac{di_a(t)}{dt} + k_b \frac{d\theta(t)}{dt} = v_s(t) \quad (4.5)$$

The DC Motor mechanical characteristics can be described using the equation below:

$$J_M \frac{d^2\theta(t)}{dt^2} + B_M \frac{d\theta(t)}{dt} = T_M(t) \quad (4.6)$$

J_M the rotor moment of inertia and B_M is the frictional coefficient.

With time the derivative of the armature current becomes negligible with relation to the motor dynamics, therefore when rearranging 4.5 to make the armature current the subject, additionally assuming k_M and k_T is equal to k this is because they are the same constant, it becomes:

$$i_a(t) = -\frac{k}{R_a} \frac{d\theta(t)}{dt} + \frac{1}{R_a} v_s(t) \quad (4.7)$$

Then substituting equation 4.7 into 4.4 after substituting that into 4.6 we finally get:

$$\frac{d^2\theta(t)}{dt^2} + \left(\frac{B_M}{J_M} + \frac{k^2}{J_M R_a}\right) \frac{d\theta(t)}{dt} = \frac{k}{J_M R_a} v_s(t) \quad (4.8)$$

The output is rotational acceleration:

$$y(t) = \frac{d^2\theta(t)}{dt^2} \quad (4.9)$$

In order to better understand the model above, equation 4.9 has to be transferred from the time domain to the Laplace domain. This will aid in obtaining the transfer function of the model.

$$\mathcal{L}\left\{\frac{d^2\theta}{dt^2} + \left(\frac{B_M}{J_M} + \frac{k^2}{J_M R_a}\right) \frac{d\theta(t)}{dt}\right\} = \mathcal{L}\left\{\frac{k}{J_M R_a} v_s(t)\right\} \quad (4.10)$$

$$s^2\theta(s) + s\left(\frac{B_M}{J_M} + \frac{k^2}{J_M R_a}\right)\theta(s) = \frac{k}{J_M R_a}v_s(s) \quad (4.11)$$

Final Laplace Transfer function is:

$$\frac{\theta(s)}{v_s(s)} = G(s) = \frac{\frac{k}{J_M R_a}}{s^2 + \left(\frac{B_M}{J_M} + \frac{k^2}{J_M R_a}\right)s} \quad (4.12)$$

The transfer function $G(s)$ is the Laplace domain representation of the DC motor. This model would serve well in terms of formulating an accurate representation of the DC motor. The only issue is, the constants are physical properties that are unknown because the DC motor bought did not have a data sheet attached. Therefore the motors bought have unknown physical features, thus the DC motors are ought to be treated as a black box.

Another possible method to obtain the model of the DC motor is by system identification. Applying a step input and monitoring the rotational velocity response. If $G(s)$ is observed again it can be seen that one of the 2 poles of the transfer function will always be zero meaning that the transfer function can be simplified to a first order system:

$$TransferFunction = \frac{A}{\tau s + 1}; \quad (4.13)$$

Where A is the gain of the system and τ is the time constant of the system. A time constant is the time it takes to reach 63% of its final form. Using the project report [17], which is a report based on modelling Dc motors, we can determine how to find the gain and the time constant of the DC Motor.

$$A = \frac{Motor_Velocity(rads/s)_final - Motor_Velocity(rads/s)_initial}{Step_input_final(V) - Step_input_initial(V)} \quad (4.14)$$

As it can be seen from equation 4.14 in order to obtain the gain of the system, we would need the initial and final of the input in terms of volts and the initial and final values of the motor velocity.

Input voltage As discussed before, the input voltage is a PWM signal from the arduino, which goes to the Motor driver to get amplified and get sent to the motors.

The SPEED variable was 80, this is to specify the duty cycle of the PWM signal as discussed before, and the resulting pulse is displayed below

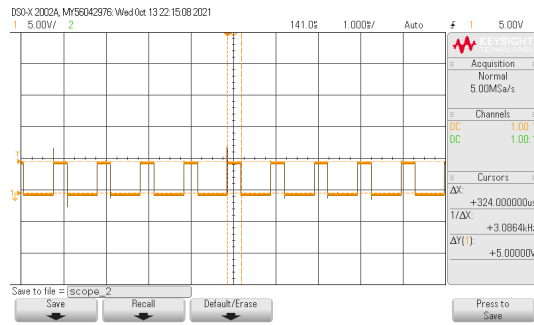


Figure 4.27: Oscilloscope reading of the PWM pin

The average voltage of this PWM signal can be calculated, as it can be seen from A.3 the PWM pins for both of the motors are pin 5 and pin 6, which means the frequency of the PWM signal is 1 Kilo Hertz signal [18] and from the 4.27 we can see that the on time is $324\mu s$. The period of the signal is $1000\mu s$. Additionally, looking at the oscilloscope it can be observed that the signal is 5 volts, using the formula below , the average voltage can be determined.

Therefore the average voltage from the figure above is:

$$\text{Average Voltage} = 5V * \frac{324\mu s}{1000\mu s} = 1.62V \quad (4.15)$$

Now that we can determine average input we can start modeling the motor. Before that, we first need to determine the deadzone of the DC Motor. The Dead Zone is the range of voltage inputs where the motor does not rotate because the input voltage is not enough to cause rotation. The proposed strategy is to increment the pwm values by 10, starting from 0 and ending at 250. and recording the rotational speed as the PWM Values increase. The code in A.4.1 illustrates how the data was collected.

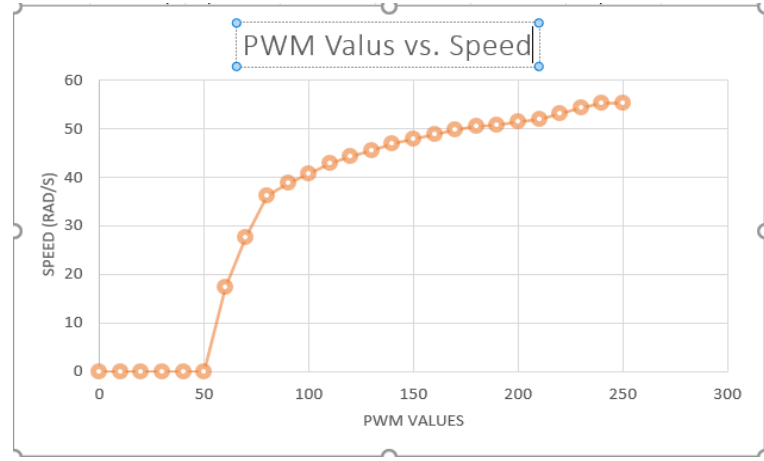


Figure 4.28: Figure of PWM values against rotational speed

From figure 4.28 it can be seen that the deadzone of the motors is from PWM values (0-50).

The step input is given and the the rotational velocity of the motor will be recorded against time. The code for the step input is provided in section A.4.2 and the ENA and ENA2 pins both that the following outputs:

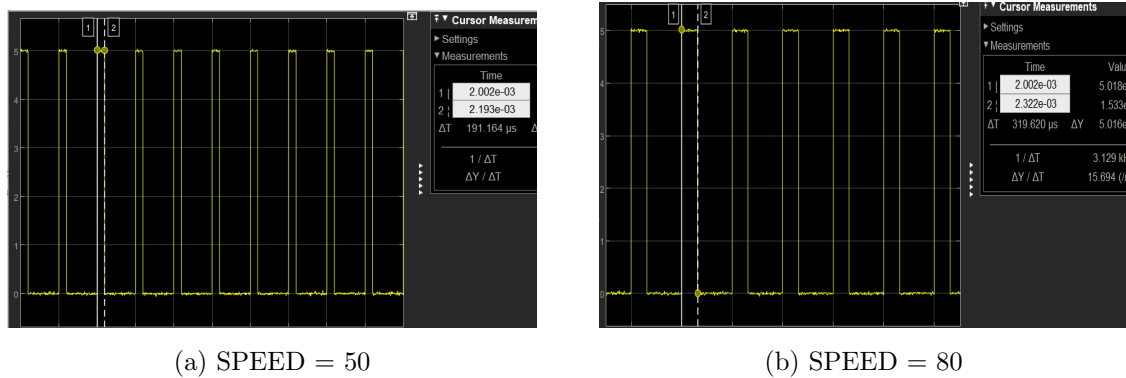


Figure 4.29: The initial and final values of the step input

As it can be seen in figure 4.29 The PWM duty cycles can by used to obtain the

average initial and final voltage as to find the voltage input using equation 4.15:

$$\text{InitialVoltage} = 5V * \frac{191.164\mu s}{1000\mu s} = 0.96V \quad (4.16)$$

$$\text{FinalVoltage} = 5V * \frac{319.620\mu s}{1000\mu s} = 1.6V \quad (4.17)$$

After this the speed of the motor was recorded and stored in a spreadsheet available in the doc. Which produced the following curve:

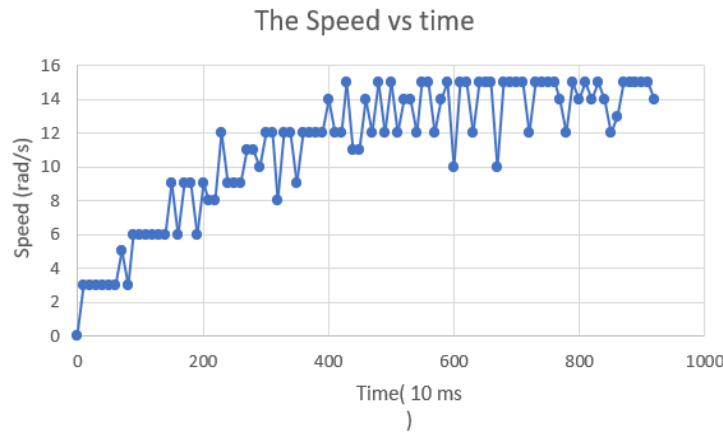


Figure 4.30: Rotational speed vs time graph

From figure 4.30 it can be seen that the plot resembles a first order response which is to be expected as discussed in the previous subsection. The data is coarse in terms of granularity but it is sufficient to determine the time constant of the plant. The final speed was 18 rad/s and 63% of 18 is 11.34 which will be rounded down to 11rad/s. The motor took 250 time steps to reach that speed which is 2.5s therefore τ is 2.5.

Since τ is known, the next thing is to determine the gain. Using equation 4.14 we

can obtain the gain:

$$A = \frac{18(\text{rad/s}) - 0(\text{rads/s})}{1.6(V) - 0.96(V)} = 28.125 \quad (4.18)$$

Finally the transfer function for the plant is as follows:

$$\text{TransferFunction} = \frac{28.125}{2.5s + 1} \quad (4.19)$$

This can be fitted into a smoother curve as shown below:

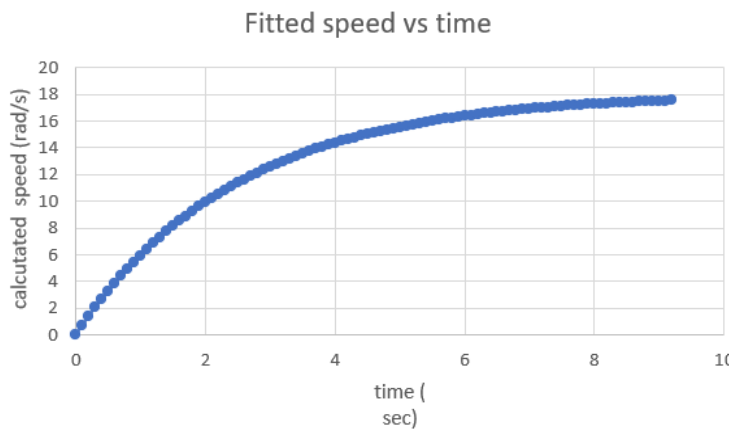


Figure 4.31: fitted Rotational speed vs time graph

Determining the distance traveled by the rig

Determining the distance traveled by the rig is fairly straight forward. as we know from the subsection 4.2.2 that the radius of the wheel is 40 mm and each revolution of the wheel covers the circumference on the ground, using this knowledge we can determine the distance travelled using the piece of code below:

```

1  float num_rot=0;
2  float dst_cov =0;
3  // distance covered and rotations covered

```

```
4     float dist,rot=0,rot_cov;
5     // the wheel radius in meters
6     float w_radius = 0.040;
7     /* Assume set up code is similar to other code snippets
       */
8     float rotation1 = (counter1 / diskslots); // calculate
                                                 RPM
9     // keeps count of the rotations covered
10    rot_cov = rot_cov + rotation1;
11    // converts the rotations covered to distance covered
12    dst_cov += 2*PI*w_radius*rotation1;
```

This snippet above determines the distance that was covered by the rig's wheel. Then how far the rig must move is the next problem to be solved. The user must enter the the distance to be covered by the rig and the distance is converted to the number of rotations to be covered and whilst the rotations covered is less than the rotations to be covered then the rig must move until the rotations covered is greater than the calculated distance. The code snippet can be found in [A.5](#) which covers what was explained above.

Chosen algorithms for motor control

There are a myriad of options in terms of controlling the motor's speed, there is open loop control and closed loop control with controller design and both of those will be explored in this section.

Open loop control This choice of control is the easiest to achieve because all that is happening is that the output of the motor which is the rotational speed is not fed back as part of the input. This means for instance, inputting a PWM value of 85 to both of the motors and letting the rig move just based on that input, for instance,

the plant transfer function 4.19 has a step response as shown in figure 4.31. we can also use Simulink to observe the response to a step input, which would represent the average voltage in a PWM input.

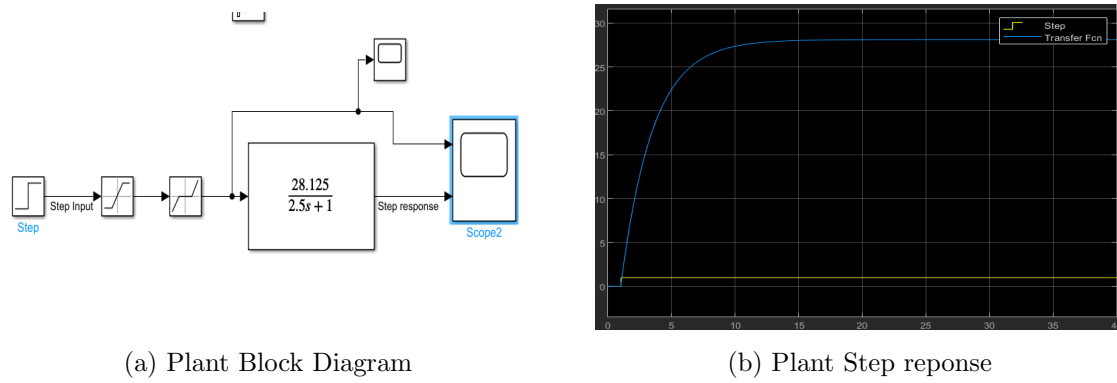


Figure 4.32: The simulation of the plant and step response

As it can be seen in figure 4.32 that the simulation of the plant response gives an appropriate view into how the motor reacts to a unit step which means that this would represent 1v average in the PWM signal, and using equation 4.16 it can be seen that the duty cycle would be about $200\mu\text{s}$ of duty cycle which is 20%. This open loop design is useful for checking the validity of the code itself and checking to see how the motors respond to PWM inputs, therefore this design will be tested and results will be recorded.

Closed loop control

This is the type of control where the output is fed back into the input by way of negative feedback. This aims to regulate the output to the plant in a way that is suitable for the application, this regulation is done by a controller and in this subsection, the controller will be designed and will be tested. The choice of controller

that will be chosen is the PID controller, this is because it is the most reliable classical controller and it is widely used in a myriad of applications as discussed in , the research displayed the effectiveness of PID control in motor speed control and thus it is a perfect fit for this particular application.

Designing the controller Before the controller is designed what can be done is place the plant in close loop and observe the response and from there, the desired response criteria can be established and then the controller will be designed according to those specifications. The open loop step response of the plant is below.

```
% creating the plant
G = tf([28.125], [2.5, 1]);
% forming a closed loop
G_cl= G/ (1+G);
% unit step input
step(G_cl)
```

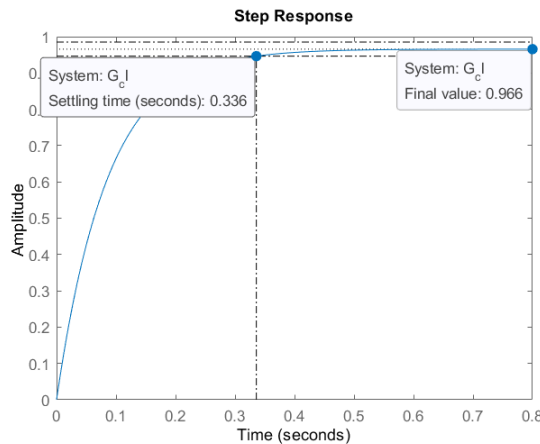


Figure 4.33: Closed loop step response

As it can be seen in the step response that the step is tracked almost perfectly which

96.6% accuracy and the settling time is 0.336s which means that the plant itself if put in close loop without any controller, it would perform very well. This Closed loop approached will also be tested, but this performance can be improved further with a controller and thus the following specifications:

- less than 20% overshoot
- less than 2% Steady State Error
- reach 98% of final value in less than 0.8s

With these specifications established, the controller can be designed. The PID controller follows this formula:

$$PID = \frac{K_p s + K_i + K_d s^2}{s} \quad (4.20)$$

Where K_p is the proportional gain, K_i is the integral gain and K_d is the derivative gain.

The close loop function for the PID controller with the plant is:

$$T = \frac{(PID)(Plant)}{1 + (PID)(Plant)} \quad (4.21)$$

which in this case turns out to be:

$$T = \frac{\frac{K_p s + K_i + K_d s^2}{s} * \frac{28.125}{2.5s+1}}{1 + \frac{K_p s + K_i + K_d s^2}{s} * \frac{28.125}{2.5s+1}} \quad (4.22)$$

After algebraic manipulation becomes:

$$T = \frac{(K_p s + K_i + K_d s^2)}{(2.5 + 28.125 K_d) s^2 + (1 + 28.125 K_p) s + 28.125 K_i} \quad (4.23)$$

This is the final closed loop transfer function for the PID controller and plant, next is to choose the poles. From the characteristic equation it can be seen that the highest order power is 2 which means two poles have to be chosen. Now since the system has to reach 98% of final value in less than 0.8s means that the time constant has to be $4\tau = 0.8$, which means τ is 0.2. Therefore one of the poles have to be further than $s=-5$ on the rootlocus. Therefore the first pole chosen is $s=-6$, the second pole will be chosen close to the origin which i choose to be $s=-0.1$ or $10s= -1$. The poles are $(s+6)(10s+1)$ and the resultant polynomical is :

$$P = 10s^2 + 61s + 6 \quad (4.24)$$

The coefficients of the polynomial are then equated with the coefficients of the characteristic equation 4.23 to obtain the gains.

$$2.5 + 28.125K_d = 10 : K_d = 0.2667 \quad (4.25)$$

$$1 + 28.125K_p = 61 : K_p = 2.1333 \quad (4.26)$$

$$28.125K_i = 6 : K_i = 0.21333 \quad (4.27)$$

The PID controller has been designed and the performance of the controller will be evaluated and decide if this improved the performance or not.

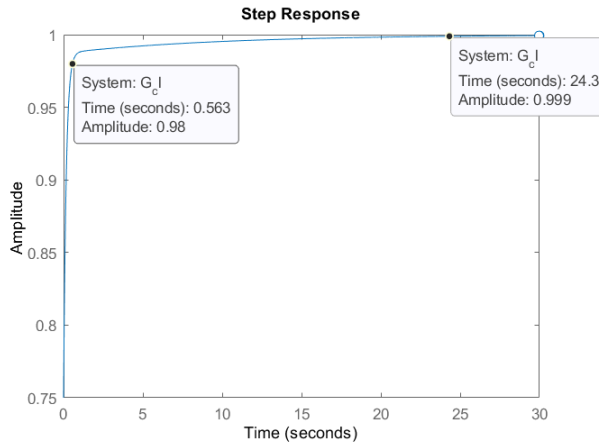


Figure 4.34: Closed loop step PID response

From figure 4.34 it can be observed that the performance of the system has worsened when which means the closed loop negative response as so far given the best performance and met most of the requirements.

Alternative Control Design Since the PID controller did not improve the performance of the plant, an alternative controller can be designed, using the closed loop plant configuration, since the most of the requirements. The steady state error can be dropped to less than 2% using just a proportional controller. Using equation 4.21 but for the proportional controller we can get the closed loop gain for the proportional controller K.

$$Gain = \frac{K * A}{1 + K * A} \quad (4.28)$$

Where A is the gain of the plant. to obtain 2% tracking error it is needed to equate the closed loop gain to 0.98, which is the final value that is needed. But to increase the accuracy, the tracking error will be set to 1.5% which means it has to be equated to 0.985:

$$\frac{K * 28.125}{1 + K * 28.125} = 0.985 \quad (4.29)$$

$$K * 28.125 = 0.985 + 27.703 * K \quad (4.30)$$

$$0.421875 * K = 0.985 \quad (4.31)$$

$$K = 2.334814815 \quad (4.32)$$

Using this gain, the following step response from the plant was obtained:

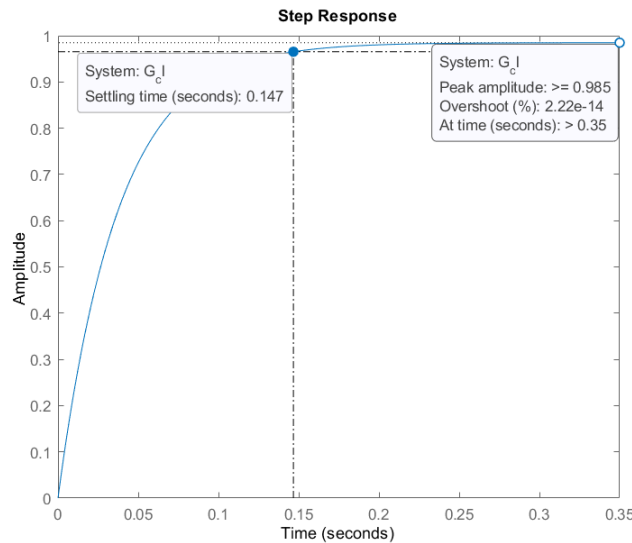


Figure 4.35: Closed loop step GAin controller response

From figure 4.35 it can be seen that the performance was greatly improved, the settling time is 0.147s, there is no overshoot and the peak response is 0.985. This is the controller that will be used moving forward.

Relating the setpoint to the output

The input to the motor is a PWM signal and the output is rotational velocity, to

relate these two using figure 4.28, the figure can be broken up into 3 sections, from (0-50) (50-80) and (80-250), these are ranges in the x-axis. These can be approximated into 3 sets of straight lines. After This, a line of regression can be fitted into the different sections and use the equation of line to relate the speed and pwm values.

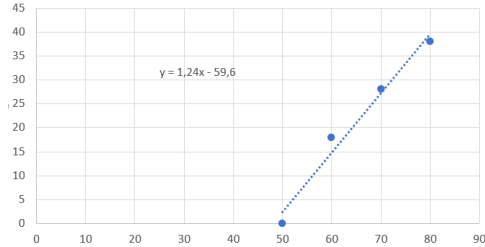


Figure 4.36: Line aprroximation of PWM(50-80) values and rotational velocity

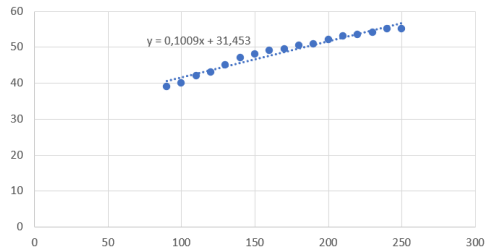


Figure 4.37: Line aprroximation of PWM(80-250) values and rotational velocity

Using these equations that are in figure 4.36 and 4.42 we can relate the speed recorded with the PWM inputs:

$$y = 1.24 * x - 59.6 \quad (4.33)$$

Equation 4.33 relates the PWM values from (50-80), x-axis being PWM values and y-axis being the rotaional velocity, so using this we can find the appropriate PWM value from recorded rotational speed. The same logic applies to PWM values (80-250).

$$y = 0.1009 * x + 31.453 \quad (4.34)$$

4.3.2 Lifting mechanism software design

The lifting mechanism will be using a pulley and scissor lift system. The pulley is powered by a servo motor which pulls the lever in the base of the scissor lift. The scissor lift base can move a length of 115.6mm as seen in figure 4.13, the side view shows the slot that the PVC pipe that is connecting the lift to the pulley, The pulley has to be able to rotate enough to fully extend the lifting mechanism. Therefore the servo is a 360 degree continuous motion. Which means that the length of the slot is the circumference of the pulley, so that the servo can rotate in one 360 degree rotation. The angles are now linked with the slot length, and the slot length is linked with the scissor lift height as explained in subsection 4.2.2. Using this information, the following can be deduced:

$$360^\circ(\text{pulley}) : 115.6\text{mm}(\text{slotlength}) \quad (4.35)$$

This relation 4.35 is link between the rotations of the pulley and how far the pipe will travel in the slot. The same relation can be made between the slot length and the scissor lift height:

$$115.6\text{mm}(\text{slotlength}) : 565.6\text{mm}(\text{liftheight}) \quad (4.36)$$

From equation 4.35 and 4.36 it can be seen how everything relates to the pulley system. Firstly, $1^\circ = 0.32\text{mm}$ (one degree of rotation equals 0.32mm movement in the slot). Secondly, $1\text{mm} = 4.89\text{mm}$ (for each millimeter moved in the slot then 4.89mm will move vertically in the lifting mechanism). This can be executed in code which can be found in Appendix A.6. This code performs the algorithms that were discussed above in order to lift the mechanism.

The main problem that needed to be solved in this algorithm was calculating the

angle that the servo motor has to turn, because the angle has been determined using the equations above. The issue is that the servo is a continuous rotation servo motor which presents a new problem because. 180° servo motors have a servo motor library in Arduino which can accept direct angle input and the servo motor will turn the inputted angle for instance, the command "myservo.write(60);;" will send a PWM signal to the servo to rotate 60°.

For continuous servo motors, there is no such correlation between the input and output instead, the input relates to the speed and direction of the servo for instance:

"myservo.write(0);;" - Causes Clockwise rotation at maximum rotation speed
"myservo.write(90);;" - Causes the servo motor to stop rotation
"myservo.write(180);;" - Causes counterclockwise rotation at maximum rotation speed

This means that the servo motor can only be turned off and on in 2 directions. Which means a new approach has to be taken to solve the angle. Which brings attention to the possibility of using the speed of the motor to determine the angle to be rotated. For instance, the speed of the servo motor chosen is (0.18s/60 degrees)- 4.8v supplied and (0.16s/60 degrees)- 6v supplied. Which means that the Servo motor will take between either 180ms and 160ms to reach a rotation of 60°.

Using this knowledge, the motor can be left to rotate for varying periods of time to obtain the desired angle. Firstly, the speed of the servo motor when 5v is supplied needs to be known to carry on solving the problem. The reason is because the Arduino supplies 5V through its PWM pins. The supply voltage and corresponding speed can be used to form an equation, which the x-axis being voltage supplied and the y-axis being the speed. Which means we have 2 coordinates - [4.8, 0.18] and [6,

0.16]. Using these coordinates, a linear equation can be formulated.

$$\text{gradient} = \frac{y2 - y1}{x2 - x1} = \frac{0.16 - 0.18}{6 - 4.8} = -\frac{1}{60} \quad (4.37)$$

Now that the gradient is known, the rest of the linear equation can be found using the following equation:

$$y = m * x + c \\ 0.16 = -\frac{1}{60} * 6 + cc \\ cc = \frac{13}{50} \quad (4.38)$$

Therefore the equation is :

$$y = -\frac{1}{60} * x + 0.26 \quad (4.39)$$

Using equation 4.40, the speed of the servo can be found when there a supply of 5v

$$y = -\frac{1}{60} * 5 + 0.26 = 0.177 \quad (4.40)$$

This means that it will take 177 ms to rotate 60°. In Arduino, the code for that would be:

```

1 // rotate the servo for 177ms and then stop it
2 myservo.write(0);
3 delay(117);
4 myservo.write(90);

```

This is the logic that is used in A.6 to rotate the servo to a desired angle.

4.4 Implementation

The following images are the different sections from section ?? which described the different components that make up the hardware design. All of the components that make up most of the hardware was Laser cut and the material is 3mm thick board

material.

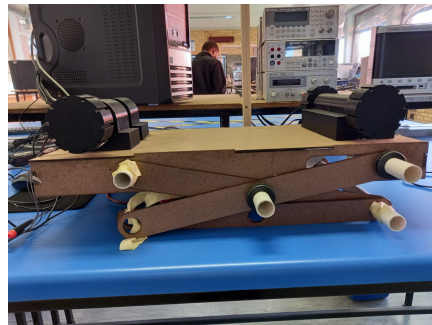


Figure 4.38: Bottom platform with the Wheels attached

Figure 4.38 shows how the back wheels and motor housing are connected, with the front wheel holders and front wheels



Figure 4.39: Lazer cut Slot

Figure 4.39 is the laser cut design of the link arms in ??



Figure 4.40: Top platform and links

Figure 4.40 is an isometric of the top platform and the rest of the linking arms.

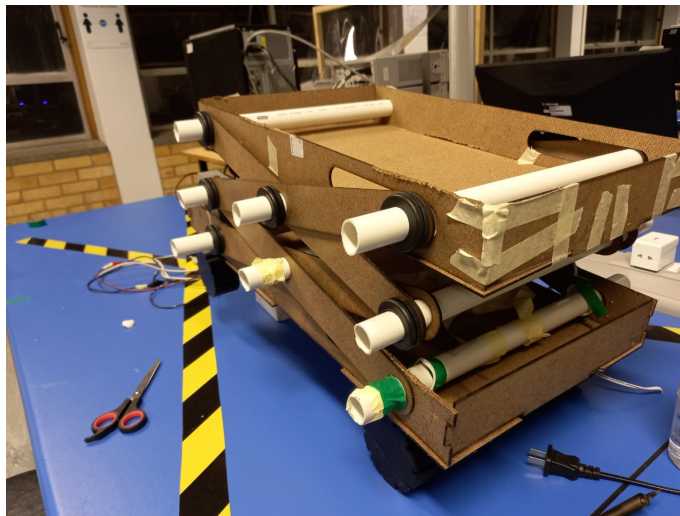


Figure 4.41: Line approximation of PWM(80-250) values and rotational velocity

Figure 4.41 illustrate the fully assembled rig

4.5 Testing

There will be 2 types of tests that will be done to validate the rig's functionality, no load and load testing. These types of tests will be done on the motor system and the lifting mechanism system.

4.5.1 Motor System Testing

No Load Testing

The no load testing is when the motors are rotating freely in a configuration similar to figure 4.38, this test is important because validates the software written, which is for the open loop testing and the closed loop testing. Different speeds and distances will be inputted and the rig should be able to run at rated speed and run for the

specified distances. The accuracy of the distance travelled will be analysed with each run.

Load Testing

The load testing is to test if the motors will run if the rig is placed on the floor and when it runs, does it travel the entered distance by the user.

4.5.2 Lifting Mechanism Testing

No Load Testing

The no load testing for the lifting mechanism is a test to see if the servo motor rotates to the correct angle when the user enters the desired lifting height. The pulley attached to the servo motor will rotate freely without the scissor lifting mechanism attached to the pulley .

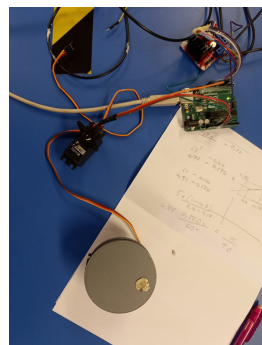


Figure 4.42: The set up for testing servo motors

Load Testing

The test is similar to the no load testing but the pulley is connected to the scissor lifting mechanism.

Chapter 5

Results

5.1 Results

The results obtained are from the testing section. The no-load tests and the loaded tests from the different subsystems of the rig we collected and in this chapter, the results of the experiments are going to be analysed and observations will be made from the results. The first results will be from no load testing of the subsystems, after that the loaded tests results will be discussed.

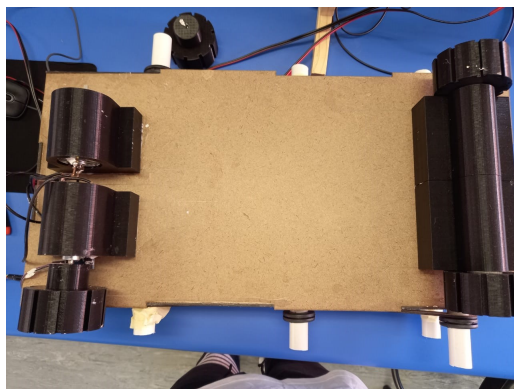
5.2 No-load testing

As explained before, no-load testing when the hardware tested is ran freely without any loads. For instance, the no-load experiments of the motor system is when the wheels of the rig run without the mass of the rig itself acting on the wheels. In terms of the lifting mechanism no-load tests, the pulley that is attached to the servo motor is not attached to anything else besides the arduino. To mainly validate the functionality of the software design. All of the data collected is available in the following Google Drive [Folder](#).

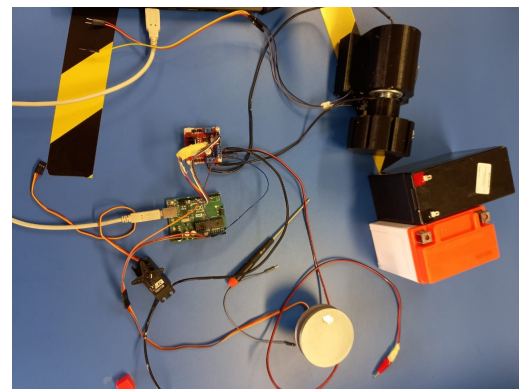
The tests were conducted the white lab and this [video](#) is the first test run. All of the following tests were ran the same way.

5.2.1 Open loop Motor system testing results

The hardware setup of the open loop experiments is shown below:



(a) Front and back wheels on the bottom platform



(b) Connection of wheels,battery, motor driver and arduino

Figure 5.1: The experimental set up for no-load motor subsystem testing

After the hardware was setup, numerous experiments were held. the aim of the experiments was observe if the motor travels the distance that the user would input. And the accuracy of the distance the wheels traveled with respect to the distance traveled.

First Run Open Loop

The first run is to make the rig travel 70 meters with a speed of 7m/s. The code snippet for the test procedure is as follows:

```
1 // distance to be travelled
```

```

2     dist = 70; //Serial.parseFloat();
3     rot = (dist/(2*PI*0.04)) // - (2*PI*0.04);
4     Serial.println("");
5     Serial.println("Enter speed of rig in (m/s) range"
6             (5.27-8.5));
7     // speed from user
8     sp = 7 ; //Serial.parseFloat();
9     // transform it to radians/second
10    sprad = sp/(2*PI*w_radius);
11    // "step input"
12    setPoint =int(sprad);
13    // Transpose to a PWM value
14    pwmsig = (int)((sprad + 59.6)/1.24);

```

The sampling of the data was 10Hz and the data recorded produced the following data in terms of speed of the motors and the distance that the wheels traveled.

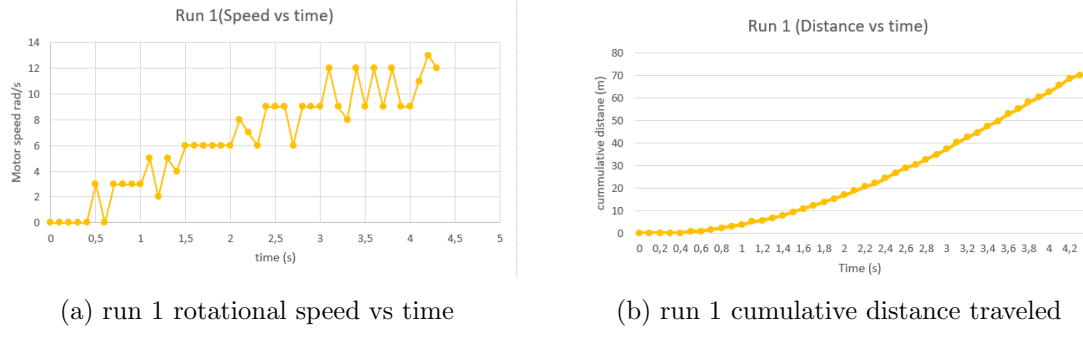


Figure 5.2: Run 1 experiment speed and distance travelled figure

Figure 5.2 illustrates the rotational speed of the wheels every 100ms and how much distance the wheels would have covered as the time passed. From the spreadsheet of the data collected, it can be seen that the rig traveled 70.03m and the time taken to

travel the distance is 4.3s

$$\text{Average Speed} = \frac{\text{distance travelled}}{\text{time taken}} = \frac{70.03\text{m}}{4.3\text{s}} = 16.28\text{m/s} \quad (5.1)$$

In terms of accuracy of distance travelled it is as follows:

$$\text{Accuracy} = \frac{\text{input distance}}{\text{distance travelled}} * 100\% = \frac{70}{70.03} * 100 = 99.957\% \quad (5.2)$$

As it can be seen the accuracy of the distance traveled is high, additionally it is less than 5 cm in terms of accuracy therefore for this run requirements for the motor system were met.

In terms of the speed of the wheels, since it is open loop therefore the response will not respond to the input speed given, which is why the speed chart has unstable speed recordings

Second Run Open Loop

For the second test, the rig was required to travel a distance of 100.2 meters with a speed of 7.2 m/s. The data was collected the same way as the first run and the following results were obtained

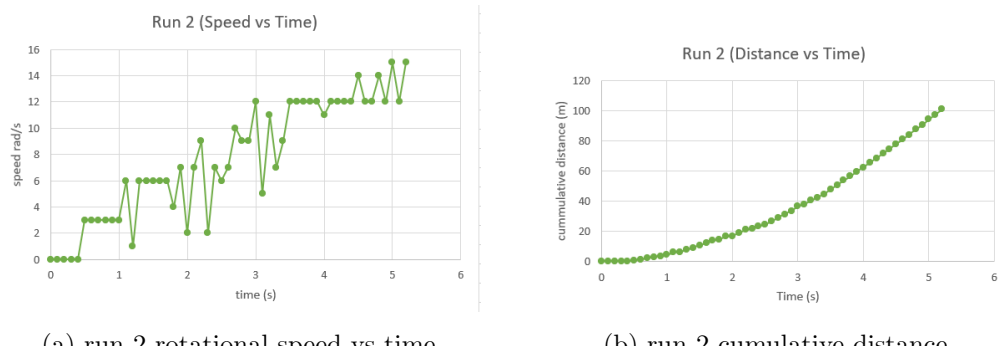


Figure 5.3: Run 2 experiment speed and distance travelled figure

From the second [Table of data](#), it can be observed that the time it took the wheels to travel that distance is 5.2 seconds. using equation [5.1](#) the average speed of the rig was 19.23 m/s. Additionally, the accuracy of the distance travelled can be calculated using equation [5.2](#). The accuracy was 99.996% .

Third run open loop

For the third experiment, the rig was required to travel a distance of 127.34 meters at a speed of 7.35 m/s.

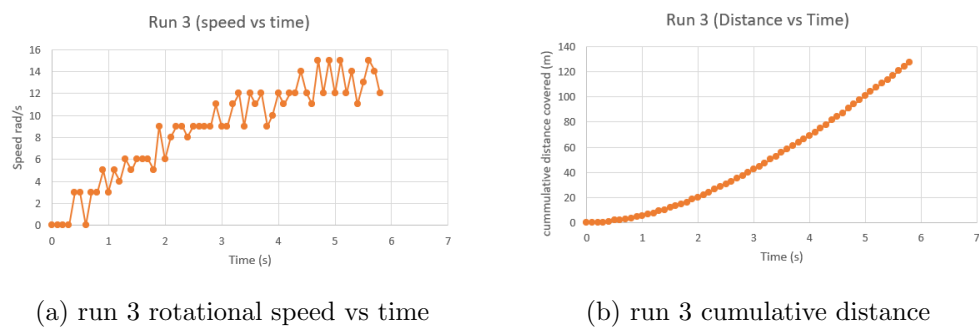


Figure 5.4: Run 3 experiment speed and distance travelled figure

The data in the third set of data shows that the rig travelled a distance of 127.4 m in 5.8s whcih means that the average speed of the rig was 21.966m/s and the accuracy of the distance covered was 99.995%. For this particular run, the deviation of the distance traveled is 6cm which is 1cm outside of the allowed deviation.

Fourth Run Open Loop

For the fourth run, the rig was required to travel a distance of 200.67m at the speed of 6.71m/s.

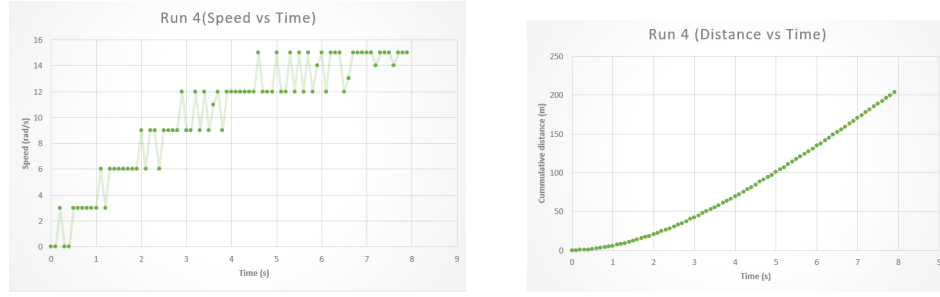


Figure 5.5: Run 4 experiment speed and distance travelled figure

In the fourth experiment, the rig traveled a distance of 200.58m in 7.9s which means that the rig was traveling at an average speed of 25.39 m/s. The accuracy of the distance travelled is 99.955%. The deviation of the distance traveled is 9cm which is 4 cm outside the range of allowed deviation.

Fifth Run Open Loop

For the fifth and final experiment, the rig was required to travel a distance of 50m at a speed of 5.92m/s.

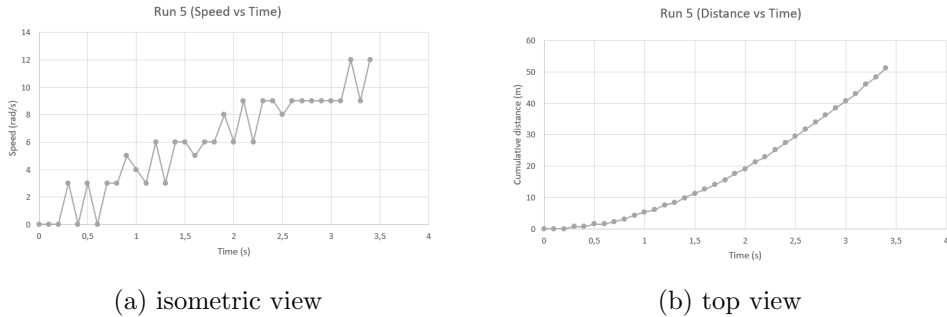


Figure 5.6: The isometric and profile view of front wheel shaft housing

The rig travelled a distance of 50.07m in 3.4s, which means it travelled at an average speed of 14.73m/s. Additionally the accuracy of the distance traveled was 99.86%

Observations From open loop results

Rotational velocity of wheels

In all of the 5 runs it can be seen that the rotational speed of the wheels is not stable. The speed of the wheels are increasing right up until the rig has reached the required distance, The ideal results of the speed graphs would be that the line that was plotted be a straight line, but instead the plots are erratic jumps into increasing speeds meaning there is acceleration and not constant velocity. Therefore in this run, the requirements of a constant voltage where not met. The closed loop experiments will aim to solve these problems raised .

Additionally, the input and the output average speed did not match instead the average speed was multiples higher than the input speed, as illustrated in the table below.

Table 5.1: Table of input and output speeds

Runs	Input speed (m/s)	Average Speed(m/s)	Deviation (m/s)
Run 1	7	16.28	9.28
Run 2	7.2	19.23	12.03
Run 3	7.35	21.966	14.616
Run 4	6.71	25.39	18.68
Run 5	5.92	14.73	8.81

Distance traveled

From the distance covered by the rig, the plots have a parabolic shape to them , which means that the rate at which the distance is covered is not constant which confirms the statement in 5.2.1. The accuracy of the distance traveled was very high, which is a positive result and majority of the traveled distances fall within the allotted range of deviation.

Table 5.2: input distance and distance travelled

Runs	Input Distance (m)	Distance traveled (m)	Deviation (m)
Run 1	70	70.03	0.03
Run 2	100.2	99.98	0.22
Run 3	127.34	127.4	0.06
Run 4	200.67	200.58	0.09
Run 5	50	50.07	0.07

5.2.2 closed loop Motor system testing results

For the closed loop motor system, the proportional controller that was designed in [4.3.1](#) was applied to the code and the existing code that was set up for the motor driving and tests which are conducted similarly to the open loop experiments. The data which produced the following sets of figures are found in a [spreadsheet](#) which is named "Closed Loop Data".

Run 1 Closed Loop Test

For this run, the rig was instructed to travel a distance of 170.77m at the speed of 5.3m/s. Which produced the following figures

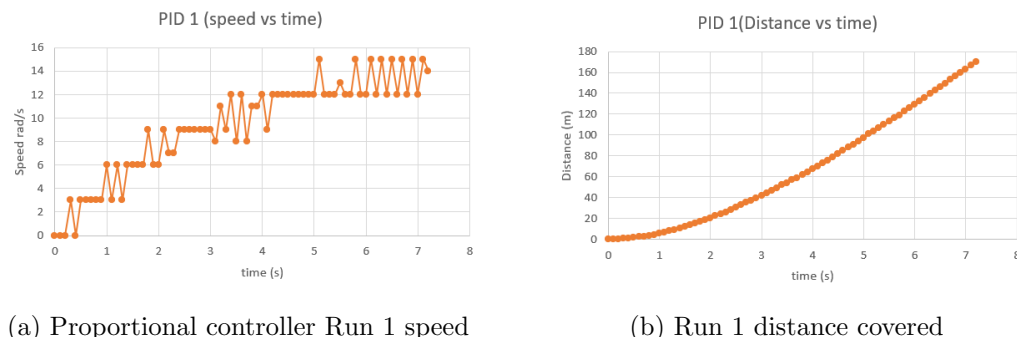


Figure 5.7: Run 1 of proportional controller Speed and distance

From the first table of sampled data it can be seen that the wheels travelled a distance of 170.71 meters and the distance was completed in 7.2s, using equation 5.1 and 5.2, the average speed of the wheels and the accuracy of the distance traveled can be calculated. The average speed was calculated to be 23.71 m/s and the accuracy of the distance covered is 99.964%. The distance that the rig travelled has deviated 1 cm more than the allotted deviation.

Run 2 Closed Loop Test

For the second test, the rig was require to travel a distance of 98.27meter at the speed of 7.5 meters and the following data was recorded:

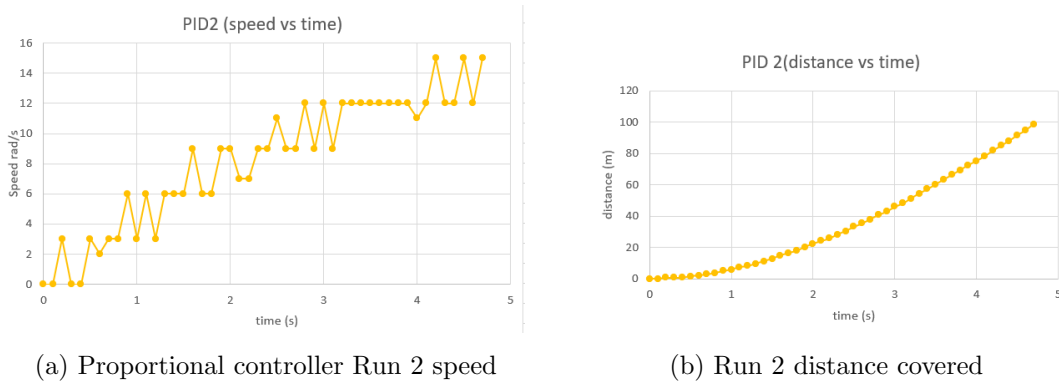


Figure 5.8: Run 2 of proportional controller Speed and distance

The rig travelled a total of 98.34 meters and that was travelled in 4.7s, which means that the rig travelled at the average speed of 20.92m/s. And the accuracy of the distance travelled is 99.93%. The distance traveled was 7cm more than the inputted distance, which is 2cm in excess of the allotted deviation.

Run 3 Closed Loop Test

For the third test, the rig was required to travel distance of 131.5 meters at the speed of 6.4 m/s.

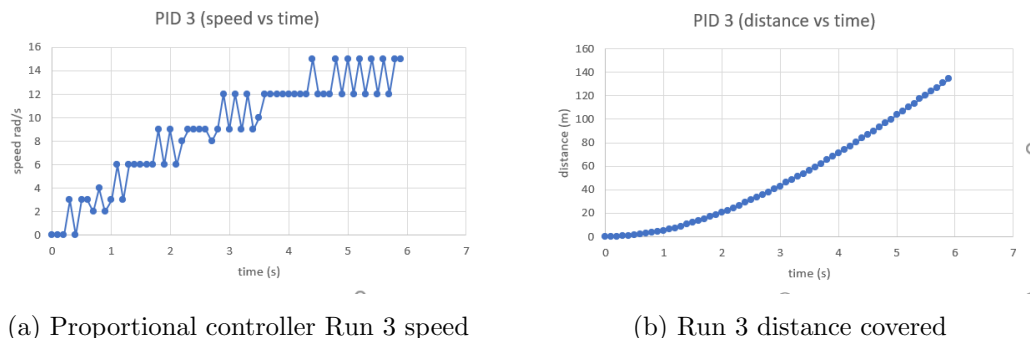


Figure 5.9: Run 3 of proportional controller Speed and distance

The rig travelled a distance of 131.46 meters and completed the distance at the

time of 5.9s. Therefore the average speed of the rig is 22.28m/s and the accuracy of the distance travelled is 99.97% with the deviation being 4cm which is within specification.

Run 4 Closed Loop Test

For the fourth experiment the rig was required to travel a distance of 198 meters at the speed of 5.6m/s and the following data was recorded

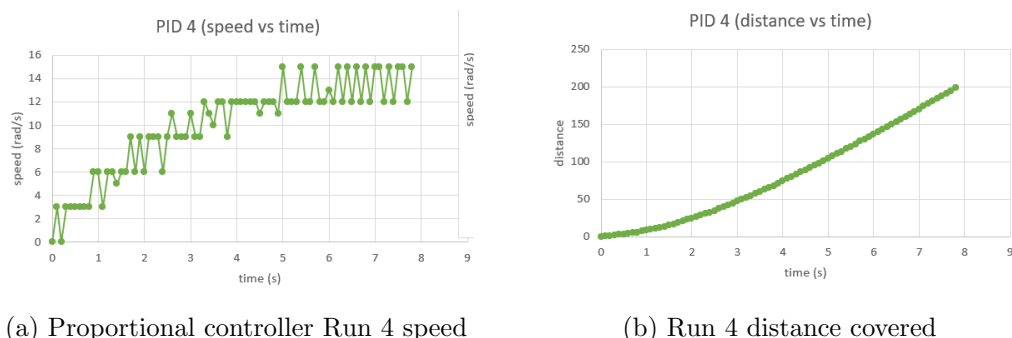


Figure 5.10: Run 4 of proportional controller Speed and distance

The rig travelled a distance of 198.05meters and the distance was covered in 7.8s, which means that the average speed of the wheels in that run was 25.39m/s and the accuracy of the distance travelled was calculated to be 99.97% .

Run 5 Closed Loop Test

For the fifth and final test the rig was required to travel a distance of 205.1 meters at a speed of 8 m/s , the following data was collected.

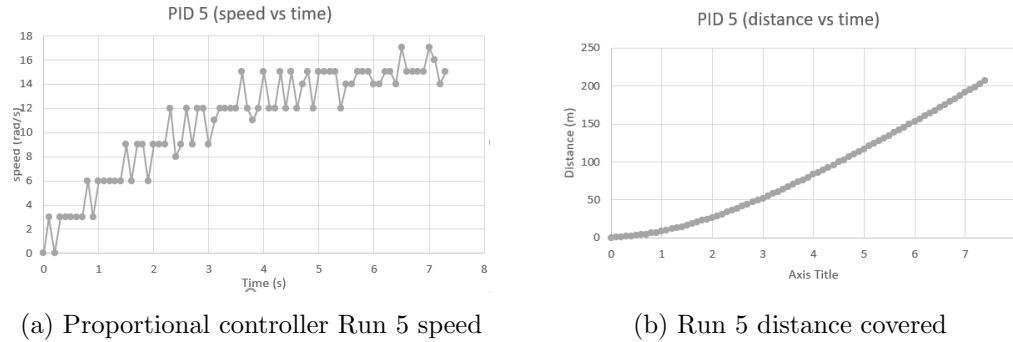


Figure 5.11: Run 5 of proportional controller Speed and distance

The rig travelled a distance of 205.09 meters and the distance was travelled in 7.4s. The average speed of the rig was calculated to be 27.715 m/s. The accuracy of the distance travelled is calculated to be 99.95%. The discussion of the results follows

Observations from closed loop tests

Distance travelled

In terms of the distance travelled by the wheels, the data displays that the accuracy of the wheels is high. as it can be seen in the table below:

Table 5.3: Distance travelled and distance input

Runs	Input Distance (m)	Distance traveled (m)	Deviation (m)
Run 1	170.77	170.71	0.06
Run 2	98.27	98.34	0.07
Run 3	131.5	131.46	0.04
Run 4	198	198.05	0.05
Run 5	205.1	205.19	0.09

As it can be seen from 5.3 that the deviation of the true distance and input distance

id all under 10 cm, this is in relation to the distances being orders of magnitude above the deviation, which in turn causes the difference infinitesimally small. Thus requirements that relate to this experiment are met.

Speed of the wheels

In terms of the recorded speed of the wheels, the speed recorded did not match up with the inputted speeds, just as in the open loop tests, which means that the control loop did not operate to specification. Though the set points did not match up, there was improvement over the open loop test results, take for instance these 2 speed graphs below:

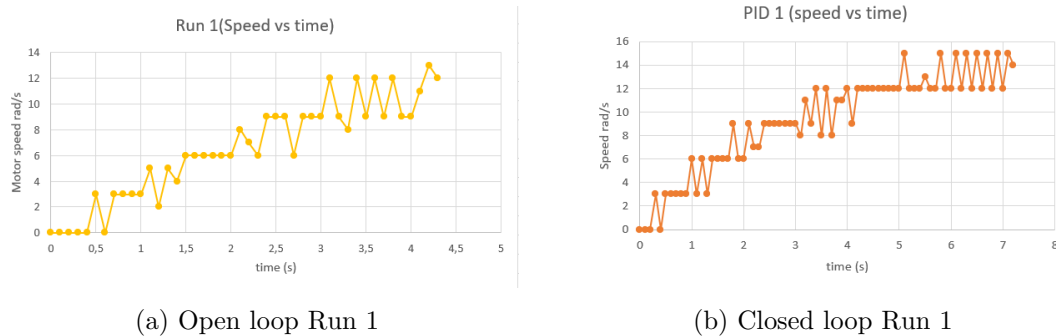


Figure 5.12: Run 5 of proportional controller Speed and distance

from figure ?? it can be observed that the graph on the right which represents the closed loop test results follows a more first order reacting , and the open loop graph seems to be more scattered. Additionally the closed loop graph maintains the same range of speeds for longer periods of time, this because the controller is actively correcting the previous speed to stabilise the next sample.

5.2.3 Lifting mechanism testing results

For this experiments, the servo was tested to observe its rotating accuracy, The input to the test was a desired height to be "lifted" by the scissor lift mechanism that would be there. after that the lifting mechanism code in A.6 performed the calculation necessary to rotate the servo motors to simulate lifting the scissor lift platform. Then the results were collected from the serial monitor and logged in a Spreadsheet named "No load lifting mechanism data" found [here](#).

A [video](#) showing how the lifting mechanism pulley was tested.

From the data collected it can be seen that there ten tests that were performed to verify the software written and to test the accuracy of the lifting mechanism. The data in the column named "Actual height from servo rotation (mm)" was calculated using the angle from the algorithm and equations 4.35 and 4.36 to obtain the absolute height, this is to observe the deviation between the calculated height and absolute angle, which is logged in the column named "Deviation".

From the "Accuracy" column it can be seen that the accuracy is at an average of 99.65% and the average deviation is 0.895mm. This means that the no-load tests meet all of the requirements relating to this experiment are met.

5.3 Loaded Testing

Load testing the system will determine the behaviour of the subsystems when there is load acting on them For instance for the motor drive system, the weight of the whole Assembly will weigh on the motors of the wheels which will affect the torque of the motors. The same goes for the lifting mechanism the links will affect the servo motors attached to the pulley.

5.3.1 Loaded Motor system testing results

As the rig was placed on the floor to test to see if the motors will have enough torque to move the rig, there was no movement in the rig at any PWM value, even the maximum 255, which is 100% duty cycle of the 12V PWM, This means that the 12V supplied by the battery did not provide enough power to the motors for them to rotate.

The following investigation was to determine the torque that the motors produce when they are at full power. In calculate the torque there nee needs to a methodology of carrying out the investigation.

Designing the test apparatus

The proposed strategy is to design a lever piece that will attach to the shaft of the motor and act as an arm. Then a known mass is attached to the arm which is a certain distance away from the shaft, and using the torque equation, the amount of torque that the motor exerts.

Arm Design

The Arm should be able to fit in the shaft of the motor and have have holes to hang weighted objects. The following design printed:

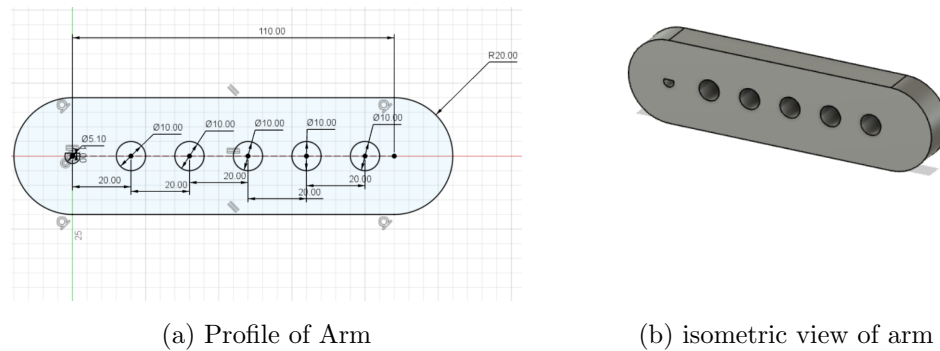


Figure 5.13: Design of the Arm

Figure 5.13 illustrates the profile view of the arm with all of the dimensions and the isometric view of the arm. The arm is 140 mm in length with 6 holes, one is for the motor shaft and the five are to hang weights from as it can be seen that the holes are 10mm id diameter and they are all equidistant from one another at 20mm.

The functionality of the arm is as follows

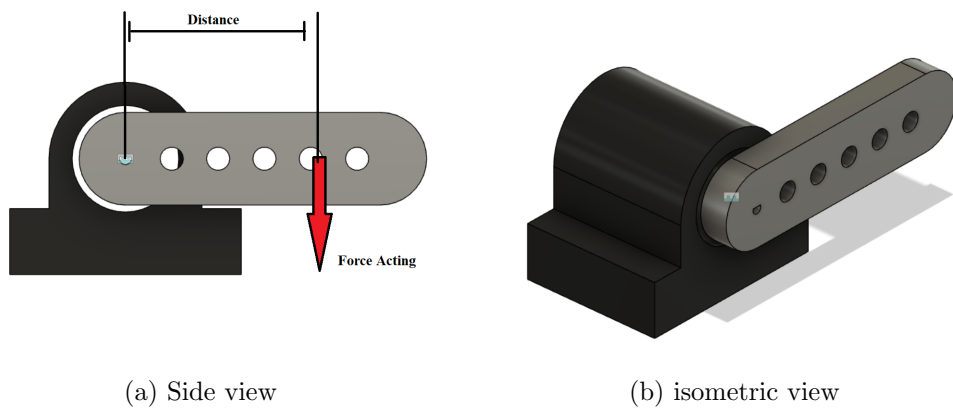


Figure 5.14: illustration of teh configuration

Figure 5.14 illustrates how the torque will be recorded. What will be done is that the motors will be run at full power and the arm has to lift the weighted objects that the arm is parallel with the horizontal. After that the following equation will be used to determine the torque:

$$\text{Torque} = \text{distance} * \text{mass} * (9.81) \quad (5.3)$$

Implementing the torque test

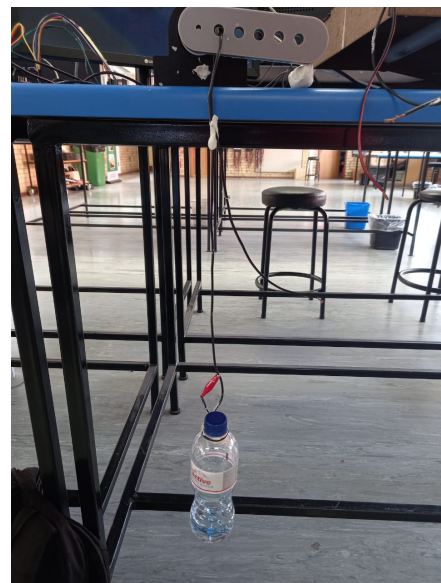


Figure 5.15: Measuring the torque

As it can be seen from figure 5.15 that there is a bottle hung from the first hole from the shaft. The bottle contained 122ml of water at room temperature, which translates to 122 g of mass, the arm itself weighs 39g and the force of the arm is assumed to act in the center of the arm at a distance of 50mm from the shaft. using

equation 5.3 we can determine the maximum torque that the motor exerts.

$$Torque = 20 * 0.122 * (9.81) + 50 * 0.039 * 98.1 = 43.065 Nmm \quad (5.4)$$

from 5.4 it can be seen that the torque is not enough to overcome the mass of the rig and the surface friction to move the rig.

Alternative Design

Due to the time constraints of the project there is not enough time to redesign the motor system or replace the motors for more powerful ones, instead what can be done is to increase the amount of power that is delivered to the motors. A second 12V battery was purchased so that the total voltage supplied to the motors is now 24V.

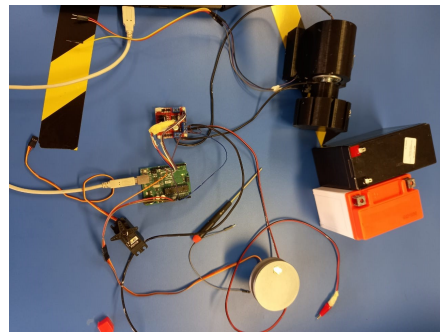


Figure 5.16: Connection of the batteries and the motors

From figure 5.17 it can be seen that there are now 2 batteries that are connected to the motors.

A maximum PWM value was applied to the motor and yet again the motors refuse to rotate when placed on the ground. This caused the motors to draw more current which overheated the motor driver, nearly destroying the arduino in the process and therefor the experiment was cut short. The next step was to determine the amount

of torque that the motors exert at that voltage. The motor could lift a bottle that weighed 337g , therefore the torque exerted was:

$$Torque = 20 * 0.337 * (9.81) + 50 * 0.039 * 98.1 = 43.065 Nmm \quad (5.5)$$

As it can be seen from 5.5, the torque is not sufficient to move the rig. Therefore it can be observed that the motors chosen did not have enough torque for this particular application.

5.3.2 Loaded Lifting mechanism testing results

For the loaded lifting platform testing the apparatus was connected in the following way:



Figure 5.17: Pulleys connected to the lifting mechanism

The pulleys did not rotate at command, the torque provided by the servo motors was not enough to lift the scissor mechanism. both of the servo motors are 13kg.cm servo

motors And the servos motors are attached to the pulleys. The radii are 18.4mm, which mean that the forquer that they exerted is calculated as follows:

$$13kg : 1cmx; 1.84cmx = 7.07kg \quad (5.6)$$

Meaning that the pulling power of each the servo motors is 7.07 kg. Therefore the pulling power of both of the servo motors is 14.13kg. Thhe test was ran again to test if the pulleys would rotate so that they can pull on the pvc pipe so that the scissor lift mechanism would lift. In this particular test, the subsystem does not pass the acceptance tests.

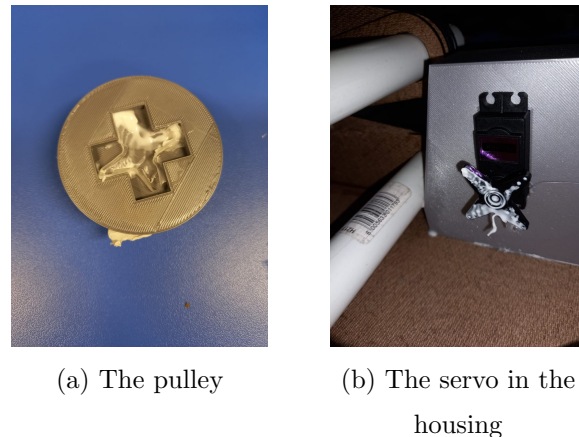


Figure 5.18: Structural failure in the lifting mechanism

As figure 5.18 illustrates, the were structural failures when the tests were conducted, as the servo motor rotated, it tore out form the pulley cavity that was made for the servo motor. This means that the pulley design had a flaw. The pulley was stuck onto the servo using cold glue, which was said to be a very strong glue but the shear forces from the servo tore the bond from the glue, resulting in this outcome

5.4 Discussion

5.4.1 No load test results

In terms of the no load tests, the hardware operated and performed as expected in terms of the Acceptance Test procedures, the sub motor subsystem met Acceptance test 2 (R.V.002) and (R.V.004), the other acceptance test procedures could not be tested because they do not apply to the motor drive subsystem.

Speed of No load tests

For the motor motor systems open loop and closed loop equations the simulated speeds of the wheels were unrealistic the table below has the average speeds of all of the runs.

Table 5.4: Speed of the motors in km/h

Open Loop tests		
Run#	Average speed m/s	km/h
Run 1	16.28	58.61
Run 2	19.23	69.23
Run 3	21.966	79.08
Run 4	25.39	91.4
Run 5	14.73	53.028
Closed Loop Tests		
Run 1	23.71	85.36
Run 2	20.92	75.31
Run 3	22.28	80.21
Run 4	25.39	91.404
Run 5	27.715	99.77

From table 5.4 it can be seen that the speeds that these experiments are running at are extremely fast for the current use-case of building a test rig for a radar system. the reason for these high speeds is because the motor is connected directly to the wheel. there is no gear reduction in place to reduce the rotational velocity of the motor.

Additionally, the reason why the speed graphs of all the experiments performed were like that was because the modelling of the speed profiles in 4.3.1, in the section where the proportional controller was designed. This is because of the way that the speed was measured in the first place. The use of 1 slot instead of the 15 slots that were design, caused the data to be less precise, resulting in very coarse data which contains a number of errors. Those errors carry through the modelling and accumulate as the design develops and this is the result of the design decisions made. Though, it must be made clear that the slot was reduced because of hardware limitations of the rotary encoder.

Distance travelled

In terms of the requirements, all of the requirements of the no load tests are met and the user requirements are also ,met, the most successful results are those of the distance that the wheels travelled. This is because they provided the most accuracy and the most consistency . The main objective of the project was to create a rig that could travel a distance of up to 50m with 5cm accuracy and the results obtained showed, that the requirement was met repeatedly and reliably.

Lifting mechanism

In terms of the no load testing for the lifting mechanism, it can be seen that the servo motor software performed as specified. Which means that in terms of the acceptance tests, the software had met the acceptance tests which means that the design was a success from this perspective.

5.4.2 Loaded Tests

In terms of the loaded tests, most of the experiment could not be ran because there were fatal design decisions that were taken in formulating a solution for the problem at hand. And as a result the loaded section of testing did not meet most of the requirements and did not pass most of the acceptance tests.

Chapter 6

Conclusions

6.1 Conclusions

The problem statement was "Testing radar technology is essential, there is a need for a mobile testing rig to test the tracking performance of radar." And the purpose of this project⁶ was to build a prototype that met the initial requirements and pass the set acceptance tests and meet user requirements. The novel solution was a design of a 4 wheeled rig which was a dual motor driven system and the platform that carries the test objects was lifted by a scissor lift mechanism. That was the proposed solution.

Despite the rig not working when it has a load on it, significant engineering problems were solved. The software for the motor drive system and lifting mechanism system is a salient accomplishment because the software will serve as a basis for all future work that would extrapolate from this research. The no-load results accomplished most of the user requirements in terms of testing functionality and validity of the design choices made throughout the project.

In terms of limitations, there were quite a few, the budget being R1500 constricted the purchasing choices, especially in terms of purchasing motors, good quality motors that have high torque would have caused an excess in expenditure, additionally, the servo motors bought could have been more powerful but that comes at an extra cost which would be outside the budget. In terms of time, there were 13 weeks allotted for the completion of this project and this time constraint restricted the depth of the project. In terms of alternative design decisions could have been taken and experimented on. Refinement of the subsystems was limited because of the time given. A large part of the time was taken by research and development of the system itself, leaving very little time to implement and iterate designs. Hence the V-model was chosen, because it followed a rigid schedule which was needed for this project. Also the rig design itself was limited by the time constraint, many iterations may have been able to be completed to refine the external design .

As stated before, one of the important positives of the project was the motor being able to travel the required distance with very high precision at high speeds

6.2 Future Work

In terms of continuing the topic, there is a foundation already set with respect to possible methodologies and design decisions made in the project. I would hope to - in iterative implementations- refine the rig design and apply more advanced speed control methods such as MPC (Model Predictive Control).

Some of the improvements that can be made in the project are:

- Motors with encoders mounted on

- High torque motors
- Alternative lifting mechanism designs
- More accurate modeling methods

Bibliography

- [1] “Working principle of dc motor,” <https://xked.com/1403/>, 2020, (Accessed on 03/09/2021).
- [2] Labman, “The magnetic force,” <http://labman.phys.utk.edu/phys222core/modules/m4/The20magneticforce.html>, (Accessed on 03/09/2021).
- [3] “Difference between stator rotor,” <https://circuitglobe.com/difference-between-stator-and-rotor.html>, (Accessed on 03/09/2021).
- [4] “Servo motor – types and working principle,” <https://www.electronicshub.org/servo-motors/>, (Accessed on 03/09/2021).
- [5] “Bldc motor,” <https://www.ato.com/bldc-motor>, (Accessed on 03/09/2021).
- [6] *HALL EFFECT SENSING AND APPLICATION*. Honeywell, 2015.
- [7] “Motor encoder overview,” https://www.dynapar.com/Technology/Encoder_Basics/Motor_Encoders/, (Accessed on 03/09/2021).
- [8] S. A. A. M. K. Alipour, “Point-to-point stable motion planning of wheeled mobile robots with multiple arms for heavy object manipulation,” in *Point-to-point stable motion planning of wheeled mobile robots with multiple arms for heavy object manipulation*. IEEE, 2011, pp. 1–6.

- [9] S. Ali, A. Moosavian, and S. S. Hoseyni, “Dynamics modeling and tipover stability of a hybrid serial-parallel mobile robot,” no. 2, pp. 1024–1029, 2002.
- [10] “Closed-loop control system,” <https://electronicscoach.com/closed-loop-control-system.html>, (Accessed on 05/09/2021).
- [11] “What is holonomic constraints?” <https://www.quora.com/What-is-holonomic-constraints?share=1>, 2019, (Accessed on 05/09/2021).
- [12] “What is a pid controller, their types and how does it work?” <https://www.electricaltechnology.org/2015/10/what-is-pid-controller-how-it-works.html>, 2020, (Accessed on 05/09/2021).
- [13] A. Iyer and H. O. Bansal, “Modelling, Simulation, and Implementation of PID Controller on Quadrotors,” in *Modelling, Simulation, and Implementation of PID Controller on Quadrotors*. IEEE, 2021, pp. 1–7.
- [14] V. A. K. Kulkarni and R. Talele, “PID Controller based DC Motor Speed Control,” in *PID Controller based DC Motor Speed Control*. IEEE, 2017, pp. 35–38.
- [15] *A QUICK INTRODUCTION TO SLIDING MODE CONTROL AND ITS APPLICATIONS*. Universita Degli Studi Di Cagliari.
- [16] S. S. S. Prabhudev Ghalimath, “,” in *Speed control of DC motor using sliding mode control approach*. IOSR-JEEE, 2015, pp. 17–19.
- [17] A. Ngwenya, “Process control and instrumentation project 2021 report,” https://vula.uct.ac.za/access/content/attachment/dd450b81-293f-4a49-a788-a91b68657f3f/Assignments/a0e92410-24eb-4e8d-a52c-926d2ec1923b/NGWAKH003_EEE4118F_FINAL%20PROJECT.pdf, June 2021, (Accessed on 29/10/2021).
-

- [18] “Arduino-pwm-frequency,” <https://arduinoinfo.mywikis.net/wiki/Arduino-PWM-Frequency>, (Accessed on 29/10/2021).
- [19] “Selecting quadcopter motor: A detailed guide 2021,” <https://robu.in/selecting-quadcopter-motor-a-detailed-guide-2021/>, (Accessed on 03/09/2021).
- [20] M. Paun, J. Sallese, and M. Kayal, “,” *Computer*, pp. 86–96, 2013.
- [21] R. A. F. E. Quintero-Manríquez, “,” in *Second-Order Sliding Mode Speed Controller with Anti-windup for BLDC Motors*. IEEE, pp. 1–6.
- [22] P. C. R. C. U. N. D. Marques, L. Perdigoto, “,” in *DC MOTORS CONTROL USING ACTIVE OBSERVERS*. Re-seacrhGate, pp. 667–672.

Appendix A

Supporting Data

Appendix sections are where you can place large figures, data tables, and spinets of code. Use appendices to your benefit to keep the body of your thesis concise!

The lyrics found below are for your enjoyment, but also serve an important role in demonstrating latex syntax for formatting text and in-text citations.

A.1 Electrical Hardware Connections

The table below shows how different components are connected to the arduino pins. The first coloumn lists the pins used and the second column lists the corresponding pins of the hardware.

Table A.1: A table of corresponding electrical connections

Arduino Pins	Hardware Connection
Pin 2. (INT 0)	LM393 Encoder (D0 pin)
Pin 5. (PWM ₁)	L298N Driver (ENA pin)
Pin 6. (PWM ₂)	L298N Driver (ENB pin)
Pin 7. (GPIO)	L298N Driver (IN 1 pin)
Pin 8. (GPIO)	L298N Driver (IN 2 pin)
Pin 9. (PWM ₃)	FS5113R Servo (Signal pin)
Pin 12. (GPIO)	L298N Driver (IN 3 pin)
Pin 13. (GPIO)	L298N Driver (IN 4 pin)
5V pin	FS5113R Servo (VCC pin) LM393 Encoder (VCC pin)
Vin	L298N Driver (+5V pin)
GND	L298N Driver (GND) FS5113 Servo (GND) LM393 Encoder (GND)
L298N Driver pins	Hardware connection
12 V pin	Battery (12V + pin)
GND pin	Battery (GND pin)
OUT 1 pin	Motor 1 +ve pin
OUT 2 pin	Motor 1 -ve pin
OUT 3 pin	Motor 2 +ve pin
OUT 4 pin	Motor 2 -ve pin

A.2 Encoder Internal circuitry

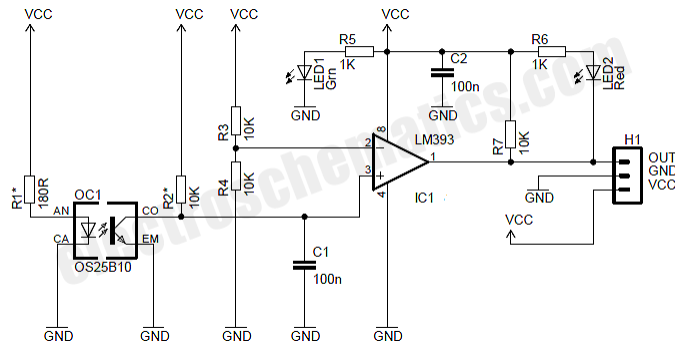


Figure A.1: Diagram of electrical connections for Lifting mechanism

A.3 Encoder-Motor Setup

```

1 // Incharge of clockwise or anti-clockwise rotation
2 int In1 = 7;
3 int In2 = 8;
4 // Setting up pins for MotorB
5 int In3 = 12;
6 int In4 = 13;
7 // PWM pin set up For MotorA and MotorB
8 int ENA = 5;
9 int ENA2 = 6;
10
11 // The speed of the motor (0-255)
12 int SPEED = 70;
13
14 // Constants for interrupt pins

```

```
15     const byte motor1 = 2; // motor  Interrupt pin - INT
          0
16
17     // Integers for pulse counters
18     unsigned int counter1 =0;
19
20     // number of slots in encoder disk
21     float diskslots = 15.00;
22
23
24     void setup() {
25         // put your setup code here, to run once:
26         Serial.begin(9600);
27         Timer1.initialize(1000000/10);
28         attachInterrupt(digitalPinToInterruption(motor1),
                           ISR_count1,FALLING); // Increase counter 1 when
                           speed sensor pin goes low
29         Timer1.attachInterrupt( ISR_timerone ); // enabling
                           the timer
30         //pinMode(13,OUTPUT);
31         pinMode(In1,OUTPUT);
32         pinMode(In2,OUTPUT);
33         pinMode(In3,OUTPUT);
34         pinMode(In4,OUTPUT);
35         pinMode(ENA,OUTPUT);
36         pinMode(ENA2,OUTPUT);
37
```

38 }

A.4 Modelling DC Motor

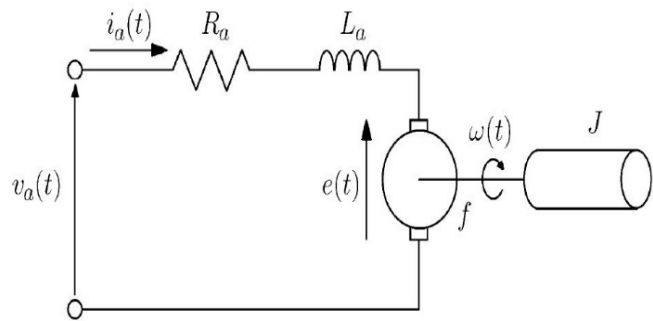


Figure A.2: Diagram of electrical diagram of DC motor

A.4.1 Deadzone code

```

1 // Setting up pins for MotorA
2 // Incharge of clockwise or anti-clockwise rotation
3 int In1 = 7;
4 int In2 = 8;
5
6 // Setting up pins for MotorB
7 int In3 = 12;
8 int In4 = 13;
9
10 // PWM pin set up For MotorA and MotorB
11 int ENA = 5;
12 int ENA2 = 6;
```

```
13 // The speed of the motor (0-255)
14 int SPEED = 0;
15
16 void ISR_timerone()
17 {
18     Timer1.detachInterrupt(); //stops the timer
19     Serial.print("Motor_Speed_-_PWM");
20     float rotation1 = (counter1 / diskslots); // calculate
21     RPM
22     Serial.print(rotation1);
23     Serial.print(",");
24     Serial.print(SPEED); // print the
25     Serial.println("");
26     counter1=0; // reset counter to zero
27     Timer1.attachInterrupt( ISR_timerone ); //Enable the
28     timer
29 }
30 void setup() {
31 // put your setup code here, to run once:
32 Serial.begin(9600);
33 Timer1.initialize(1000000/10); // frequency of printing
34 to the serial monitor
35 attachInterrupt(digitalPinToInterruption(motor1),
36 ISR_count1,FALLING); // Increase counter 1 when speed
37 sensor pin goes low
38 Timer1.attachInterrupt( ISR_timerone ); // enabling the
39 timer
```

```
34 //Setting the pins up as outputs
35 pinMode(In1,OUTPUT);
36 pinMode(In2,OUTPUT);
37 pinMode(In3,OUTPUT);
38 pinMode(In4,OUTPUT);
39 pinMode(ENA,OUTPUT);
40 pinMode(ENA2,OUTPUT);
41 }
42
43 void loop() {
44     // clockwise rotation
45     while (SPEED<251) {
46         digitalWrite(In1,HIGH);
47         digitalWrite(In2,LOW);
48         analogWrite(ENA,SPEED);
49         digitalWrite(In3,HIGH);
50         digitalWrite(In4,LOW);
51         analogWrite(ENA2,SPEED);
52         SPEED = SPEED + 20;
53     }
54 }
```

A.4.2 Step input

```
1     SPEED = 50;
2     // run the motors clockwise
3     digitalWrite(In1,HIGH);
```

```
4     digitalWrite(In2,LOW);
5     analogWrite(ENA,SPEED);
6     digitalWrite(In3,HIGH);
7     digitalWrite(In4,LOW);
8     analogWrite(ENA2,SPEED);
9     wait for 1 second
10    delay(1000);
11    // increase PWM value, which increases average
12    voltage
13    SPEED = 80;
14    analogWrite(ENA,SPEED);
15    analogWrite(ENA2,SPEED);
```

A.5 Distance covered by rig code snippet

```
1 void rigcontrol(){
2     dst_cov =0;
3     rot_cov =0;
4     Serial.println("Enter_Distance_to_be_covered_in_meters
5         ");
6     while (Serial.available() == 0) {
7         // Wait for User to Input Data
8     }
9     // converts user input to a float
10    dist = Serial.parseFloat();
11    // converts the distance to number of rotations to be
12    covered
```

```
11    rot = dist/(2*PI*0.04);
12    // checks to see if the distance is greater than zero
13    if(dist >=0){
14        // whilst rotations is greater than rotations covered
15        // then this loop is true
16        while(rot>rot_cov) {
17            digitalWrite(In1,HIGH);
18            digitalWrite(In2,LOW);
19            analogWrite(ENA,SPEED);
20            digitalWrite(In3,HIGH);
21            digitalWrite(In4,LOW);
22            analogWrite(ENA2,SPEED); }
23
24
25    dst_cov =0;
26    rot_cov =0;
27    digitalWrite(In1,LOW);
28    digitalWrite(In2,HIGH);
29    digitalWrite(In3,LOW);
30    digitalWrite(In4,HIGH);
31    delay(5);
32    digitalWrite(In1,LOW);
33    digitalWrite(In2,LOW);
34    digitalWrite(In3,LOW);
35    digitalWrite(In4,LOW);
36 }
```

A.6 Lifting Mechanism Code snippet

The code for the lifting mechanism and the motor drive system is available at

[This GitHub](#)

Application for Approval of Ethics in Research (EiR) Projects
Faculty of Engineering and the Built Environment, University of Cape Town

ETHICS APPLICATION FORM

Please Note:

Any person planning to undertake research in the Faculty of Engineering and the Built Environment (EBE) at the University of Cape Town is required to complete this form **before** collecting or analysing data. The objective of submitting this application *prior* to embarking on research is to ensure that the highest ethical standards in research, conducted under the auspices of the EBE Faculty, are met. Please ensure that you have read, and understood the **EBE Ethics in Research Handbook** (available from the UCT EBE, Research Ethics website) prior to completing this application form: <http://www.ebe.uct.ac.za/ebe/research/ethics1>

APPLICANT'S DETAILS		
Name of principal researcher, student or external applicant	Akhile Ngwenya	
Department	Electrical Engineering (EBE)	
Preferred email address of applicant:	NGWAKH003@myuct.ac.za	
If Student	Your Degree: e.g., MSc, PhD, etc.	Bsc(eng) Mechatronics
	Credit Value of Research: e.g., 60/120/180/360 etc.	40 Credits
	Name of Supervisor (if supervised):	Dr Francois Schonken
If this is a researchcontract, indicate the source of funding/sponsorship		
Project Title	Design of a Low Radar Cross-Section Rig for Controlled Motion of a Calibrated Radar Target	

I hereby undertake to carry out my research in such a way that:

- there is no apparent legal objection to the nature or the method of research; and
- the research will not compromise staff or students or the other responsibilities of the University;
- the stated objective will be achieved, and the findings will have a high degree of validity;
- limitations and alternative interpretations will be considered;
- the findings could be subject to peer review and publicly available; and
- I will comply with the conventions of copyright and avoid any practice that would constitute plagiarism.

APPLICATION BY	Full name	Signature	Date
Principal Researcher/ Student/External applicant	Akhile Ngwenya		16 Aug. 21
SUPPORTED BY	Full name	Signature	Date
Supervisor (where applicable)	Dr. WPF Schonken		18 Aug 2021

APPROVED BY	Full name	Signature	Date
HOD (or delegated nominee) Final authority for all applicants who have answered NO to all questions in Section 1; and for all Undergraduate research (Including Honours).			

Figure A.3: Ethics

Akhile Ngwenya - Electrical Engineering